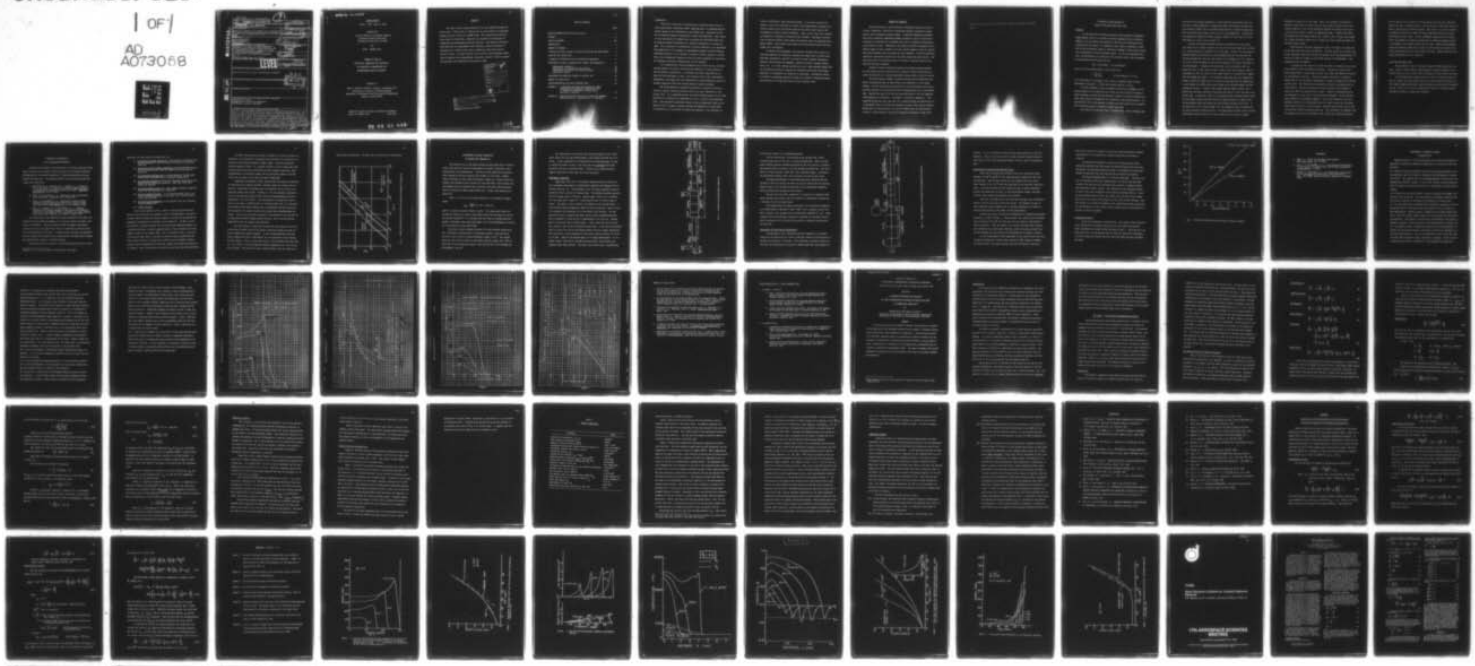
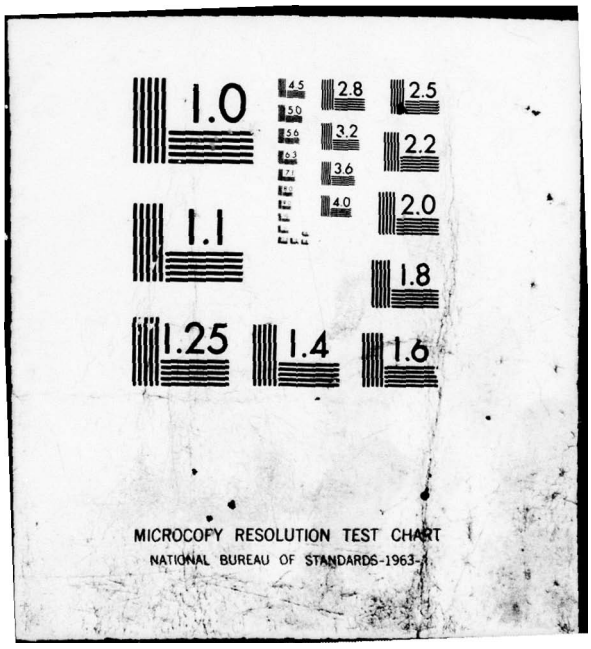
AD-A073 058 ILLINOIS UNIV AT URBANA-CHAMPAIGN DEPT OF AERONAUTICA--ETC F/G 21/2
INITIATION, COMBUSTION AND TRANSITION TO DETONATION IN HOMOGENE--ETC(U)
JUL 79 R A STREHLOW, H O BARTHEL, H KRIER AFOSR-77-3336

UNCLASSIFIED AFOSR-TR-79-0934 NL

1 OF 1
AD A073058



END
DATE FILMED
9-79
DDC


1.0
1.1
1.25
1.4
1.6
1.8
2.0
2.2
2.5
2.8
3.2
3.6
4.0
4.5
5.0
5.6
6.3
7.1
MICROCOPY RESOLUTION TEST CHART
NATIONAL BUREAU OF STANDARDS-1963-A

UNCLASSIFIED

SECURITY CLASSIFICATION OF THIS PAGE (When Data Entered)

REPORT DOCUMENTATION PAGE

READ INSTRUCTIONS BEFORE COMPLETING FORM

1. REPORT NUMBER: AFOSR-TR- 79-0934	2. GOVT ACCESSION NO.
3. RECIPIENT'S CATALOG NUMBER	
4. TITLE (and Subtitle): INITIATION, COMBUSTION AND TRANSITION TO DETONATION IN HOMOGENEOUS AND HETEROGENEOUS REACTIVE MIXTURES.	5. TYPE OF REPORT & PERIOD COVERED: INTERIM rept. 1 Jun 78 - 31 May 79
6. PERFORMING ORG. REPORT NUMBER	
7. AUTHOR(s): ROGER A. STREHLOW, HAROLD O. BARTHEL, HERMAN KRIER	8. CONTRACT OR GRANT NUMBER(s): AFOSR-77-3336
9. PERFORMING ORGANIZATION NAME AND ADDRESS: UNIVERSITY OF ILLINOIS AT URBANA-CHAMPAIGN, AERONAUTICAL AND ASTRONAUTICAL ENGINEERING DEPT, 101 TRANSPORTATION BLDG., URBANA, IL 61801	10. PROGRAM ELEMENT, PROJECT, TASK AREA & WORK UNIT NUMBERS: 2308A1, 61102F
11. CONTROLLING OFFICE NAME AND ADDRESS: AIR FORCE OFFICE OF SCIENTIFIC RESEARCH/NA, BLDG 410, BOLLING AIR FORCE BASE, D C 20332	12. REPORT DATE: July 1979
	13. NUMBER OF PAGES: 71
14. MONITORING AGENCY NAME & ADDRESS (if different from Controlling Office)	15. SECURITY CLASS. (of this report): UNCLASSIFIED (12) 53p.
	15a. DECLASSIFICATION/DOWNGRADING SCHEDULE

LEVEL II

16. DISTRIBUTION STATEMENT (of this Report)

Approved for public release; distribution unlimited.

17. DISTRIBUTION STATEMENT (of the abstract entered in Block 20, if different from Report)

DDC RECEIVED AUG 23 1979 C

18. SUPPLEMENTARY NOTES

19. KEY WORDS (Continue on reverse side if necessary and identify by block number)

NONIDEAL BLAST WAVES
DEFLAGRATION TO DETONATION TRANSITION
INITIATION OF GASES TO EXPLOSION

20. ABSTRACT (Continue on reverse side if necessary and identify by block number)

This short interim report summarizes the work completed during the period 1 June 1978 to 31 May 1979 for the Air Force Office of Scientific Research as part of Grant No AFOSR 77-3336. The research deals with the broad topics of initiation, combustion and transition to detonation in homogeneous and heterogenous reactive mixtures. One specific area deals with analytical and experimental work directed to direct initation of detonation by a nonideal blast wave in chemically sensitized reactive fuel-air clouds. The other specific topic involves the hydrodynamic modeling of ignition and flamespreading in granular energetic solids to predict the potential for deflagration-to-detonation (DDT).

DD FORM 1 JAN 73 1473

176 005

AD A073058

DDC FILE COPY

AFOSR-TR- 79-0934

INTERIM REPORT

[June 1, 1978 - May 31, 1979]

Prepared for

Air Force Office of Scientific Research
Aerospace Sciences Directorate
Bolling Air Force Base, DC 20332

for

Grant: AFOSR77-3336

SUMMARY OF WORK ON INITIATION, COMBUSTION AND TRANSITION TO DETONATION IN HOMOGENEOUS AND HETEROGENEOUS REACTIVE MIXTURES

Prepared by

Roger A. Strehlow, Harold O. Barthel, and Herman Krier
University of Illinois at Urbana-Champaign
Department of Aeronautical and Astronautical Engineering
Urbana, Illinois 61801

Approved for public release; distribution unlimited
Grant No. AFOSR77-3336 July 1979

79 08 22 049

ABSTRACT

This short interim report summarizes the work completed during the period June 1, 1978 to May 31, 1979 for the Air Force Office of Scientific Research as part of Grant No. AFOSR77-3336. The research deals with the broad topics of initiation, combustion and transition to detonation in homogeneous and heterogeneous reactive mixtures. One specific area deals with analytical and experimental work directed to direct initiation of detonation by a nonideal blast wave in chemically sensitized reactive fuel-air clouds. The other specific topic involves the hydrodynamic modelling of ignition and flamespreading in granular energetic solids to predict the potential for deflagration-to-detonation (DDT).

Accession For
NTIS GRA&I
DDC TAB
Unannounced
Justification
By
Distribution/
Availability Codes
Dist | Avail and/or special
A

AIR FORCE OFFICE OF SCIENTIFIC RESEARCH (AFSC)
NOTICE OF TRANSMITTAL TO DDC
This technical report has been reviewed and is approved for public release IAW AFR 190-12 (7b).
Distribution is unlimited.
A. D. BLOSE
Technical Information Officer

79 08 22 049

TABLE OF CONTENTS

Page

REPORT DOCUMENTATION PAGE (DD Form 1473). i

ABSTRACT. ii

TABLE OF CONTENTS iii

INTRODUCTION. 1

SUMMARY OF PROGRESS 3

A SYNOPSIS OF WORK RELATED TO FUEL/AIR INITIATION AND BLAST WAVES . . 5

PLANS FOR THE COMING YEAR 8

A SYNOPSIS OF RESEARCH ON DDT OF GRANULATED PROPELLANT. 9

EXPERIMENTS TO OBTAIN INFORMATION ON DYNAMIC BED PERMEABILITY 13

Experimental Apparatus 14
Limitations of Experimental Measurements 16
Experimental Procedures and Planned Testing. 18
Preliminary Results. 19

IMPROVEMENTS IN NUMERICAL SCHEMES TO PREDICT DDT. 22

SUMMARY OF PUBLICATIONS 29

TALKS/PRESENTATIONS ON AFOSR SPONSORED WORK 30

APPENDIX A: A SEPARATED TWO-PHASE FLOW ANALYSIS TO STUDY DEFLAGRATION-TO-DETONATION TRANSITION (DDT) IN GRANULATED PROPELLANT by Herman Krier and James A. Kezerle. 31

APPENDIX B: DIRECT DETONATION INITIATION BY LOCALIZED ENHANCED REACTIVITY by H. O. Barthel and R. A. Strehlow. 62

INTRODUCTION

The direct initiation of detonation by a localized source such as a laser pulsed spark, capacitance spark, exploding wire, or exploding high explosive charge is well understood at the present time. Initiation by the use of localized chemical accelerators is much less understood. Here, there is still the question of whether one can generate an initiating shock wave by using the proper distribution of a chemical accelerator in a source region. Also, nonlinear, two-dimensional initiation behavior is not understood. The proposed work will encompass an experimental program in which nonlinear initiation behavior will be studied in systems of direct interest to the Air Force, and a theoretical program in which the basic mechanisms of initiation by localized accelerator concentrations will be explored.

It is expected that these developments will justify the use of direct testing required to discover the initiation behavior of a wide variety of fuel-accelerator combinations. It therefore has direct applicability to Phase III FAE development as well as the studies of fuel tank vulnerability. Furthermore, the program will have application to understanding the nature of nonideal explosions that occur during explosive release accidents.

The DDT phenomenon in granulated propellant or explosives involves a series of complex transient processes that are not well understood at the present time. It is hypothesized that the normal burning process of the solid propellant is disturbed by an abnormality such as a crack in the propellant grain. This abnormality generates regions of porous propellant which can be ignited locally, causing a pressure buildup and formation of a weak shock. If detonation is to be excited following this ignition, it is necessary to

ensure a sufficiently rapid pressure buildup. In the case of porous propellant, this may be achieved as a result of the penetration of gaseous combustion products into the interior pores of the solid, which leads to the disturbance of surface burning conditions. Thus, in this case, heat transfer by conduction is replaced by convective heat transfer. Subsequent acceleration of ignition (flame) fronts begins and pressure waves are generated which become shocks. These shocks cause large local over-pressurization and often change into a detonation.

To analyze this phenomenon, the reactive two-phase (solid, gas) conservation equations of continuity, momentum and energy must be solved along with many constitutive relations to account for heat transfer interaction, pressure losses through the aggregate, ignition criteria, unsteady burning rates, etc. It is only through solutions of such a fluid-mechanics model that one can develop criteria to specify the conditions under which the burning propellant is susceptible to transition to detonation. Considerable effort is involved in developing numerical integration schemes to adequately handle the prediction of strong shock waves in such transient flows.

SUMMARY OF PROGRESS

During this period, study continued on phenomena associated with initiation, combustion, transition to detonation (DDT) and attenuation in homogeneous and heterogeneous reactive media. A modified Lagrangian time-dependent finite difference (Oppenheim (CLOUD)) program was used to study direct initiation of detonation by a nonideal blast wave in chemically sensitized reactive fuel-air clouds. Modeling of the Arrhenius kinetics throughout the explosion region in such a manner as to also satisfy computer stability requirements and reasonably short run times has been completed. Testing of different sensitizer concentration profiles in the source region has been started. The shock tube study of initiation using a 15° ramp on a splitter plate at the back wall has been completed.

Studies of flame acceleration processes by obstacles placed between two flat plates has been started as have studies of flame acceleration processes by obstacles in a layered combustible mixture which is open at the top.

The fluid dynamics needed to predict deflagration-to-detonation transition in granulated beds of high energy solid propellant is still being modeled. We have determined the sensitivity of the inter-phase viscous drag and heat transfer on the predictions of the flamespreading rate in such packed beds. Some of the results of this work were published in the 17th Symposium (International) on Combustion. The paper is included as Appendix A. Also completed during this past year were (a) a detailed design and fabrication of an experiment that will provide the necessary pressure drop relation through packed beds of solid particles, as would be needed under the high pressure convective flow conditions, and (b) new numerical integration schemes that

allow for calculations to include severe shock wave buildup in the DDT model.

A SYNOPSIS OF WORK RELATED TO FUEL/AIR INITIATION AND BLAST WAVES

PROGRESS

In the theoretical initiation program we have adapted the Oppenheim CLOUD program, which is a constant time step Lagrangian finite difference scheme, so we can examine the question of what type of distribution of accelerator must be present in a spherical source region to generate a shock wave in the surrounding region of sufficient strength to cause direct initiation of detonation in the surrounding region. For our now completed first case, the distribution of accelerator had a uniform central core surrounded by a decreasing concentration given by

$$F(R) = F_1[\cos(3\pi\delta) - 9.0\cos(\pi\delta]/16.0$$

where F_1 is the concentration in the central core,

$$\delta = \frac{R_o - R}{R_o - R_1} \qquad \text{for the range } R_1 \leq R \leq R_o,$$

R_1 is the radius of the central core, and R_o is maximum radius at which accelerator is present. In this first case we made $R_1 = 0.2\ R_o$.

We first attempted to use an Arrhenius kinetic law throughout the explosion region, but we found the use of this law led to rates of energy addition becoming so large that the numerical stability criterion required very small time steps and consequently the computation time became excessive. We then modified the law by imposing a maximum rate which could not be exceeded and in addition imposed a minimum allowable time step.

The program now runs well with no instabilities. After verifying that

we could run the program adequately, we have modified the Arrhenius rate law such that at high temperature it adequately models the methane oxidation process and below 1000°K, has an extremely high effective activation energy such that the reaction just cannot occur at all at room temperature. The high and low temperature regimes are flared together smoothly so that there is no discontinuity in a plot of log k versus 1/T.

We have successfully obtained detonation initiation for cases where the central core is highly reactive out to 0.2 of its full radius and is flared as a cosine function of reactivity out to the edge. We have also successfully obtained detonation initiation in the surrounding gas for the case when the flaring extended over only six cells (from cell 46 through cell 51.) However, if we use a bursting sphere for the central region we do not get initiation in the surroundings. It appears from the output of the calculation that the reason for this is that when the central region reacts very rapidly, inertial containment of the very center of the region causes it to explode more rapidly than the neighboring region. The resulting compression wave has temperatures within it which are higher when it reaches the core edge than the temperature is just behind the initial shock wave created by the bursting sphere and thus initiation can occur. Further, the minimum required energy release rate is greater for the short reactivity transition zone than it is for the wider transition zone. In addition, there is the possibility that extremely large values of core energy release rates may cause the compression wave to change into a fully-developed shock wave before the wave reaches the edge of the core. If the shock wave is not strong enough, then the temperature may be insufficient to cause initiation outside the core. The implication of these results is that sufficiently rapid reaction of a central region in the cloud can trigger

detonation irrespective of its shape. This is an important consideration because it means that one need not be too fussy about the shape of the core reactive region in order to get detonation provided the energy release rate in the reactive region is within an appropriate range. Shaping does affect the minimum required energy release rate, however, with a larger value needed for a short transition region than is needed for a wide transition region for the same initial shape.

The nonlinear initiation experiments using a 15° ramp at the back wall of the shock tube were quite unsuccessful. For some reason we were never able to get reasonable smoke track records and because of the two-dimensionality of the flow we made no attempt to take streak records of the phenomenon. That program has been terminated.

A program has been started to study the effect of obstacles in the path of the flame on flame acceleration processes. Initially we used two flat plates placed about 2 inches apart and blew very large soap bubbles of methane-air stoichiometric mixtures. These were ignited centrally as cylindrical bubbles and in some preliminary experiments a variety of obstacles were placed in their path. The obstacles were cylindrical obstacles surrounding the ignition source. Obvious accelerations occurred because of the increase in noise level when the obstacles were in place. However, instrumentation was not developed to record any of the acceleration phenomena. We have recently again shifted our experimental emphasis. We are now planning to run an experiment in which a two-dimensional flame is allowed to pass over two-dimensional objects between two glass plates. Schlieren observations will be used to record the flame acceleration processes. This experiment is different from the previous one in that the chamber which contains the combustible mixture

will be open at the top and will be only partially filled with combustible mixture by using a layering process. The point here is that free clouds are open at the top and are heavily layered. Thus we feel it is more realistic to examine acceleration by obstacles under conditions which more closely match those in real clouds. Various rectangular obstacles will be placed across the chamber at different spacings and at different heights relative to the height of the layered portion of the cloud. Repetitive photographs using the schlieren system will be taken to observe both the motion of the cloud and the motion of the flame inside the cloud. Optimum conditions for flame accelerations will be looked for.

PLANS FOR THE COMING YEAR

The systematic study of initiation using the CLOUD program will continue. After a rather complete understanding of methane initiation is obtained we plan to look at other fuels by putting in their kinetic rate laws.

In the experimental program we plan to study in some detail the effect of various sized and shaped obstacles on the acceleration process of a free flame propagating through a layered combustion mixture which is open at the top. This is a strictly two-dimensional study so it should be easily amenable to analysis by hydrocode techniques.

A SYNOPSIS OF RESEARCH ON

DDT OF GRANULATED PROPELLANT

Work has been underway at the University of Illinois these past three years to analyze the unsteady reactive two-phase flow associated with DDT (Deflagration to Detonation Transition) of confined granulated solid propellant and explosives. The modeling efforts to date which have been published are listed below:

1. Beckstead, M. W., Peterson, N. L., Pilcher, D. T., Hopkins, B. D., and Krier, H., "Convective Combustion Modeling Applied to Deflagration-to-Detonation Transition of HMX", Combustion and Flame 30, 231-241 (1977).

2.* Krier, H. and Kezerle, J. A., "Modeling of DDT in Granulated Solid Propellant", AFOSR-TR-78-07, October 1977.

3. Krier, H. and Gokhale, S. S., "Modeling of Convective Mode Combustion through Granulated Propellant to Predict Detonation Transition", AIAA Journal 16, 177-183 (February 1978).

4. Krier, H., Gokhale, S. S., and Hoffman, S. J., "Unsteady Two-Phase Flow Analysis Applied to Deflagration-to-Detonation Transition", AIAA Paper 78-1013, presented at the 14th AIAA/SAE Joint Propulsion Conference, Las Vegas, NV (July 1978).

The formulation of the theoretical models presented in the above list indicates the continuing development of the analysis which can predict transition to detonation. From the countless number of computer simulations carried out we have determined that there are constitutive relations which are "rate-determining" functions. In addition these relations are generally not well defined for unsteady flows at high pressure and high solids loading - the regime of most interest to the DDT problems.

The key constitutive relations, in some representative order of their

---

*Appendix A is a technical paper extracted from this report.

importance (as they affect the predictions) are:

(1) Gas-particle viscous interaction, which basically determines the hot-gas permeability into the unignited portions of the granulated bed.

(2) Gas-particle heat transfer coefficient, which determines the convective energy transfer from the turbulent flow hot gases to particles.

(3) The propellant burning rate at extreme pressures (of the order of 10^9 nt/m^2) and rapid rates of pressure change, dp/dt.

(4) The ignition criteria that fixes the time that the particles are ignited by the convective processes. Heat flux rates often exceed 10^9 watts/m^2.

(5) The intergranular stress that, under highly transient conditions, limits the (extreme) particle compaction.

(6) The gas equation-of-state. It has been determined that a constant co-volume correction to the ideal e.o.s. is not valid at these high pressures.

(7) The temperature dependency on the specific heat, gas viscosity, and gas conductivity.

(8) A DDT criterion.

In the study reported in Ref. 4 above, we have noted that the gas-particle drag interaction, as generally used in the DDT models, can lead to sizeable particle motion and extreme compaction, unless one can provide the appropriate intergranular resistance to the compaction. In short, it was not possible to properly predict the convective mode combustion dynamics in long granulated beds, using the same gas-particle drag interaction law that seemed to work for the shorter beds. And as discussed in Ref. 4, the data base that has been used to correlate the pressure drop in packed beds has been carried out both at steady-state conditions and at Reynold's numbers several orders of magnitude less than that needed for the DDT flow processes. In addition, these correlations were based on tests only with inert particles.

The same criticism must obviously be applied to the heat transfer coefficient, as correlated at low pressures and relatively low velocities, resulting in only moderate Reynold's number ranges. From the sensitivity studies reported in Refs. 2-4, a general conclusion can be stated that both the gas-particle friction coefficient and heat transfer coefficient, when extrapolated to the Reynold's number and low porosities needed in the DDT flows, are too large, by at least one order of magnitude.

Propellant and explosive linear burning rates are generally expressed as functions of the ambient pressure, through a power law steady-state correlation. Measurement of burning rates are generally never carried out at pressures greater than 10,000 - 20,000 psi. Yet the pressures predicted to occur in the confined granulated bed during the flamespreading can exceed 250,000 psi ($1.72\ (10^9)$ nt/m^2). And the pressure can change with time at rates of the order of 1000 psi/μsec to 10,000 psi/μsec! Thus it is questionable whether steady-state burning rates, extrapolated from much lower pressures,represent the dynamic burning rates during these flamespreading processes. Also, the gas velocities relative to the particles can vary from 10 to 1000 meters/second, bringing unknown factors, such as erosive burning augmentation into the burning rate expression.

One also requires an ignition criterion from the stimulus of the convective heat transfer from the hot gaseous combustion products as they are forced through the unignited regions. It was already mentioned that heat fluxes ranging from 100 to 1000 BTU/in^2 sec are calculated to occur during the DDT process. Little, if any, data exist at these extreme flux rates that tie into either a critical propellant surface temperature or a critical ignition energy. With these flux rates, ignition delay times are often less

than several microseconds. No data exist to verify such a possibility.

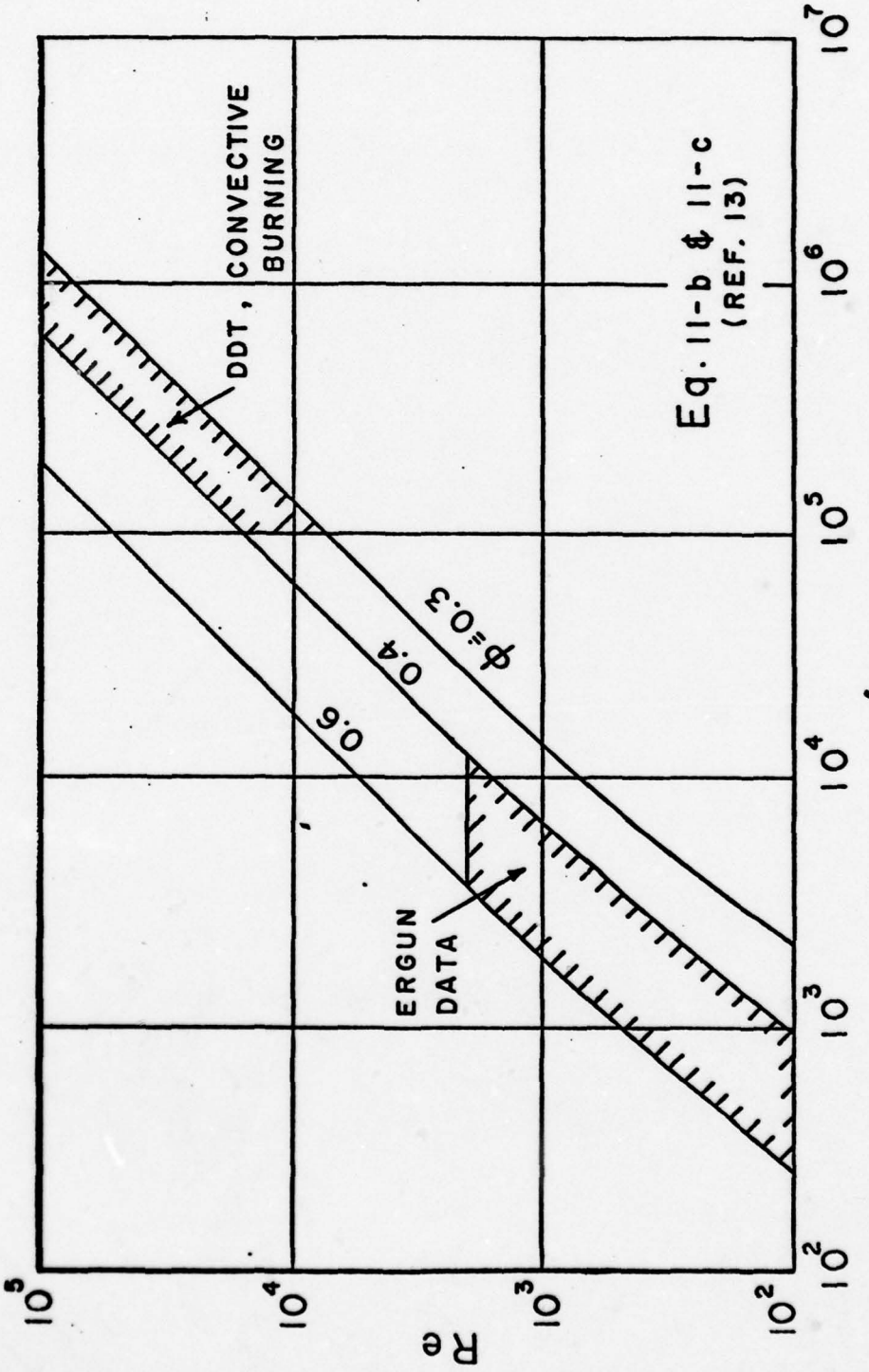


Fig. 1. Packed Bed Gas-Particle Friction Correlation According to Ergun [5].

EXPERIMENTS TO OBTAIN INFORMATION ON DYNAMIC BED PERMEABILITY

The pressure loss of the gases flowing through packed beds of various sized solid particles has been investigated by numerous researchers, both theoretically and experimentally. The work of Sabri Ergun [5] has generaly been accepted as the most accurate and reliable in this field. However, Ergun's findings are only valid for Reynold's number, Re, (based on particle diameter and superficial gas velocity) of less than 3000. More recently, Kuo and Nydegger [6] have measured flow resistances with small particle packed beds for a Reynold's number range between 500 - 15,000, with porosity averaging 0.38.

Figure 1 is a plot of the drag coefficient, as correlated by Ergun, namely,

$$f_{pg} = \frac{(1-\phi)}{\phi^2} \{1.75\ Re + 150(1-\phi)\}$$

where ϕ = porosity (percent volume of voids). The regime where Ergun correlated his relation is shown in the figure along with the region of interest for the DDT conditions. It is obvious that one would be extrapolating well beyond a reasonable range when using Ergun's (or even Kuo/Nydegger's) relation for the gas-particle drag coefficient.

Even more recently, Robbins and Horst [7] have measured steady-state flow resistances in packed beds at much higher pressures than used in References 5 and 6 and up to values of Reynold's number of 10^5. They indeed found that the friction factor at the higher Reynold's number ($Re \sim 10^5$) was about 50% of the extrapolated Ergun's value [5] and 85% of the extrapolated Kuo/Nydegger value [6].

Our experimental test facility was already designed, but not fabricated, about the time when Robbins/Gough's work became available for us to review. In the experiment to be described in the following pages, we hope to verify the results of Ref. 7 and also carry out nonsteady flow tests. The first test rig is described below. We have only a limited pressure range to work with at this time, as will be discussed.

Experimental Apparatus

Using ideas from those investigators having previously carried out flow resistance measurements an experimental apparatus was designed and constructed (See Fig. 2). The preliminary tests are being conducted using compressed air from a battery of storage tanks. The maximum obtainable pressure from the storage tanks is 450 psig. Bourdon gage 1 (Fig. 2) is a Solfrunt 4.5" test gage with a range of 0 - 1000 psig and with a ±0.25% of span accuracy. This gage is used to monitor the pressure in the storage tanks. A Grove Pressure Reducing Regulator, Model 82-829 (720 psig max. inlet), allows us to regulate the compressed air to the desired test pressure. The compressed air enters a plenum tank which contains three straightening grids. This is designed to bring the gas to approximately zero velocity. Bourdon gage 2 is the same type as Bourdon gage 1. Gage 2 indicates the test pressure, which is used in the calculation of mass flow. At the end of the plenum tank is a Sonic Flow Nozzle from American Meter Division, Singer Corporation. This nozzle has a throat diameter of 0.375 inches (and an accuracy of ±0.15% at 10 psig). Opposite the Bourdon gage 2 is an Omega Thermocouple. It is a chromel Alumel, CASS-18G-12, grounded junction probe, that provides fast response under high pressures. The Sonic nozzle opens into a straightening

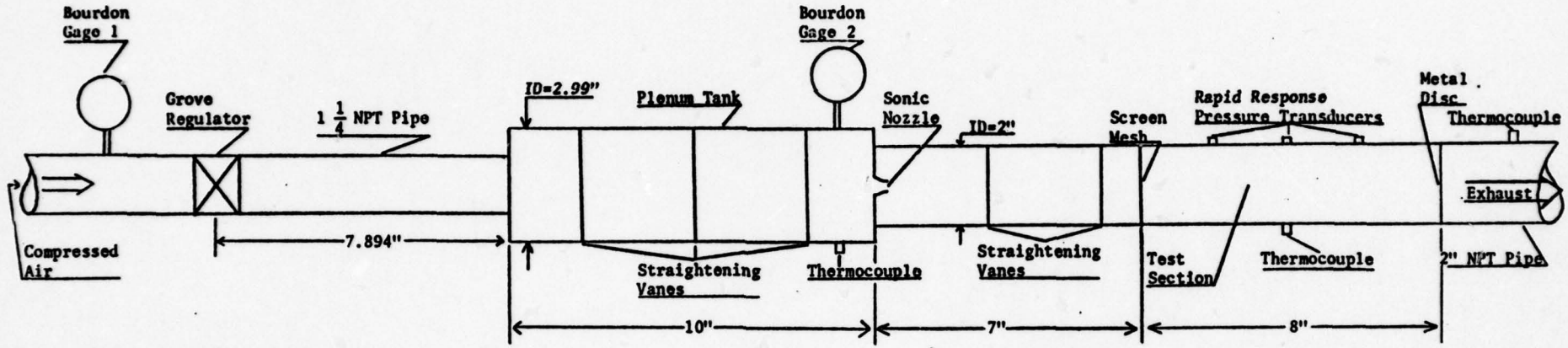


Fig. 2. Two-Phase Flow Experimental Apparatus.

section that contains two straightening grids.

The test section has a screen mesh at the entrance and a metal stainless steel grid at the exit, to hold the packed bed. There are three rapid response pressure transducers mounted on the test section, to measure the pressure drop of the gas as it flows through the packed bed. The transducers are Setra Systems', Model 205, with a pressure range 0 - 500 psig, a one millisecond response time, and an accuracy of 0.11% at full scale.

The Omega thermocouple, as described previously, monitors the temperature in the test section and after the gas has exited the test sections. Figure 3 gives a more detailed description of the experimental apparatus from the plenum tank through the test section.

The data from the Setro transducers is recorded on a Tektronix 5100 series Storage Oscilloscope, and the displays are permanently recorded with a Tektronix C-5 Oscilloscope Camera.

The readings from the Omega Thermocouples are individually displayed on an Omega Digital Thermometer, Model 2160A, with a response time of less than 2 seconds, and a maximum error including NBS conformity of ±1°F. These readings and the Bourdon gage readings are recorded in a lab book, and are used in conjunction with the Sonic flow nozzle to calculate the mass flow for each test.

Limitations of Experimental Measurements

The experimental data obtainable from this apparatus is currently limited by the compressed air source of 450 psig, which in reality gives us a workable test pressure of 400 psig. This limitation on pressure limits the flow rate and consequently the Reynold's number range that can presently be

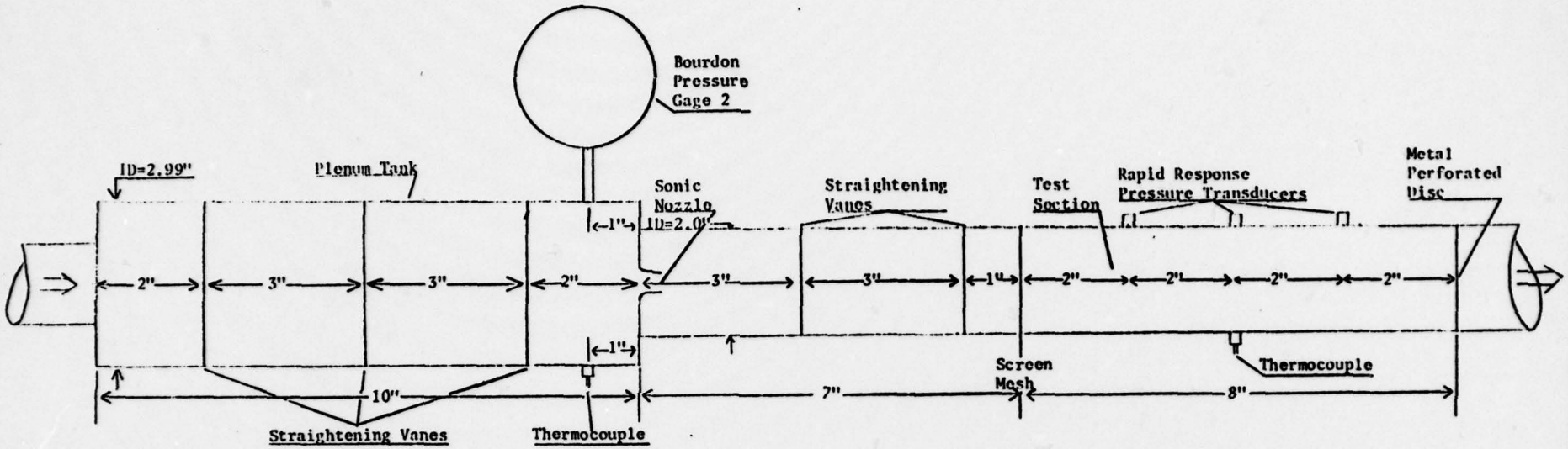


Fig. 3. Detail Dimensions of Two-Phase Flow Experimental Apparatus.

studied. It is not possible to obtain heated, high pressure air with this apparatus. Hence we are not now able to study the heat transfer and pressure drop of a hot, high pressure gas which, in fact, exists in propellant beds.

Experimental Procedures and Planned Testing

Tests will be carried out initially with 3 mm, solid glass beads (density $2.73(10^{-3})$ g/mm^3) at four input pressures, namely 100, 200, 300 and 400 psig. Then the test section will be repacked with 6 mm, glass beads (density $2.587\ (10^{-3})$ and flow conditions at the same four input pressures. The collected data will be analyzed so that a valid correlation between the coefficient of drag, f_s, and the Reynold's number, and hence the mass flow, density and porosity can be derived.

Lead shot, the same size as the 3 mm and 6 mm beads, but of different density, will be also used in the test section. The effects, if any, of these different density spheres will be studied, enabling us to better understand the parameters that affect the bed permeability.

During these tests, the pressure transducers will initially be mounted vertically, as shown in Fig. 3. Then the whole test section will be rotated first by 90° and then 180° (so that they will be located on the bottom of the test section). This will enable us to analyze the flow under identical test conditions from three axial locations, which will help us ensure that the flow through the test section and the packing of the beads is uniform.

In the second phase of this experiment we will pack the bed with inert cylindrical propellant, 0.4026 inches long and 0.18332 inches in diameter and repeat tests at the same pressures used for the spherical particles.

This latter study will attempt to verify the observations made by Robbins and Gough [7] on the geometrical scaling of particles on the bed resistance.

Our planned third phase is to mix the 3 mm beads and the inert cylindrical particles and then record the pressure drop in the bed versus the percent of spherical/cylindrical mixing, to determine any correlation between the pressure drop with the porosity and percent size mixing.

The fourth proposed phase is a transient experiment. This will consist of attaching several gas, high pressure, air bottles one inch down stream of the regulator and allowing the gas bottles to completely empty from 2000 psig to about 15 psig. The recording of the transient pressure at each of the three transducers would indicate nonsteady effects. A plot of this transient pressure drop, Δp, should cross the plot of the steady-state Δp at the various test pressures of 400, 300, 200 and 100 psig. This will enable us to check the validity of our coefficient of drag correlation for the unsteady flow case, which is what actually occurs in packed beds of interest in the DDT problems.

Preliminary Results

We are just beginning to take data now. Our initial results from the tests conducted for Δp versus mass flow of air lie within the data presented by Robbins and Gough [7] and are shown in Fig. 4. Note that our 6 mm beads which are a little smaller than 1/4 inch (or 4/16) used in Reference 7, provide conditions between the 3/16" and 5/16" bead size data of Robbins and Gough.

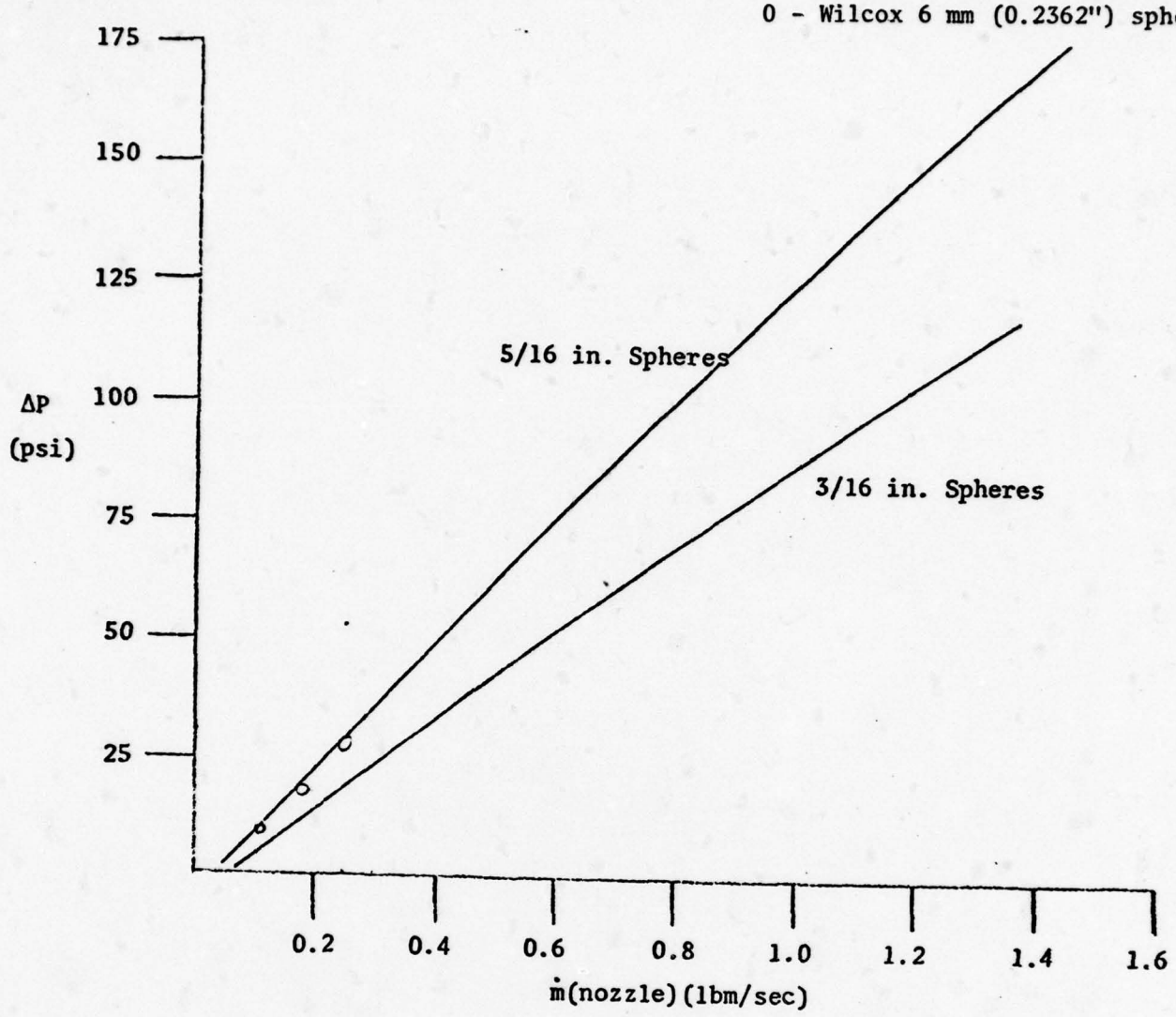


Fig. 4 Pressure Drop Versus Mass Flow Rate in Beds of Spheres

REFERENCES

5. Ergun, S., "Fluid Flow Through Packed Columns", Chem. Engr. Progr. 48, 89 (1952).

6. Kus, K. K. and Nydegger, C. C., "Flow Resistance Measurement and Correlation in a Packed Bed of WC-870 Ball Propellants", J. Ballistics 2, 1 (1978).

7. Robbins, F. and Gough, P. S., "An Experimental Determination of Flow Resistance in Packed Beds of Gun Propellant", Proc. 15th JANNAF Combustion Meeting, Newport, RI (September 1978).

IMPROVEMENTS IN NUMERICAL SCHEMES TO PREDICT DDT

Summarized below is a brief description of our efforts and progress in improving the numerical integration scheme which is utilized to solve the DDT model.

(1) Instead of using the operator form for the governing equations we are anticipating a shock to develop as transition from deflagration to detonation occurs. The simplest form of the Rankine-Hugoniot relations uses the conservation variables, namely, ρ, ρU, ρE that satisfy the jump conditions. Hence the usage of conservation variables is anticipated to produce better results.

(2) We have also revised the manner in which we specify the boundary conditions at the closed end. The correctness of the boundary conditions for such cases is insured by satisfying zero gradients at the end walls.

(3) For the predictions of deflagration to detonation transition, we have prescribed initial conditions so that the problem is sure to start as a weak deflagration. Uniform pressure, temperature and loading density will lead to the zero velocity profile which will be consistent with the governing equations. The problem is started with a perturbation in the particle energy by assuming a certain fraction of bed being ignited at initial time.

(4) An attempt was made to understand sensitivity of the constitutive relations for the particle-particle interaction force and its bearing in the particle energy equation. This is very important in view of the fact that we assume that the particle phase represents a continuum. There is only a limited data base that is available to verify predictions of particle.

heating to the compression of granular beds under high pressure.

(5) The numerical method which we have used so far is the same one we have reported previously, i.e., an explicit, two-step, predictor-corrector MacCormack method. In the current study the shock is not dealt with any special treatment. This method can be termed as a shock smearing technique. Since the governing equations are inviscid in nature, it is necessary to incorporate damping to insure numerical stability. Due to the higher non-linearity and interdependent phase quantities, we found it necessary to use artificial viscosity similar to Von Neumann and Richtmyer type all the time. After trying out various types of damping functions we found that the three point weighted average is relatively easy to use and provides quite satisfactory predictions. Figure 5 shows the pressure distribution at various times for a typical case. It shows a gradual steepening of the pressure wave which could lead to a strengthening of the shock. Figure 6 shows loci of various fronts. As could easily be seen, the flame front is accelerating moderately throughout the last half portion of the propellant bed.

(6) We are in the process of developing another differencing analog, Lax-Wendorff. It is not as yet adequately tested and hence the results are not reported in this memo.

(7) We also attempted nondimensionalizing all of the governing equations. Due to the interdependency of the two phases this poses great difficulties and only limited success in solution of the equations.

(8) We are also in the process of developing difference analog for multi-size particles. In the finished stage our DDT computer program will have the capability to handle a wider variety of problems with the propellant

particles of various sizes, as well as greater solids loadings. Even though the logic of developing such a program is fairly straightforward, with the usage of two-dimensional storage arrays, such a code poses difficulties. Most notable among them are the definitions and the distribution of the interphase transfer quantities such as drag and heat transfer. There is also a problem in defining the ignition front through multisize reactive particles. Additional insights are needed in order to make this analog successful. Figures 7 and 8 demonstrate the results of our initial efforts in developing the multisize particle program. Figure 7 indicates that much higher pressures occur at the corresponding times for the multisize particles as compared to unisize particles. Figure 8 shows the locus of flame front for the two cases.

(9) In the past our attempts were restricted to fixed space Eulerian mesh. During this research year we intend to develop a Lagrangian formulation which would allow us rezoning and restructuring the mesh depending on the strength of the shock. If this technique is successful, we should be able to clearly predict a detonation which follows from an accelerating deflagration through a porous reactive bed of propellant.

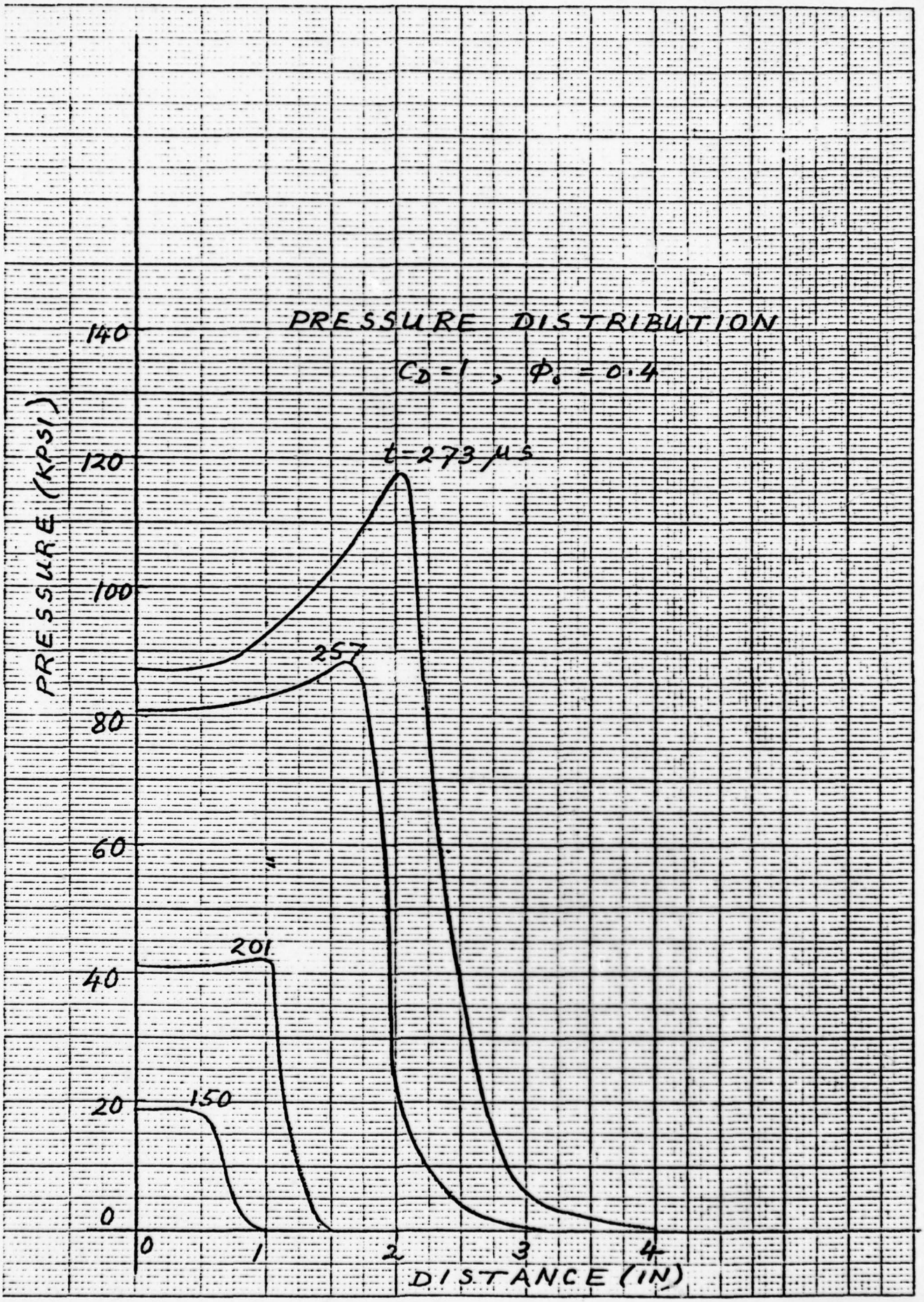

PRESSURE DISTRIBUTION
$C_D = 1$, $\phi_0 = 0.4$
t=273 μs
257
201
150
PRESSURE (KPSI)
140
120
100
80
60
40
20
0
0
1
2
3
4
DISTANCE (IN)

FIGURE 5

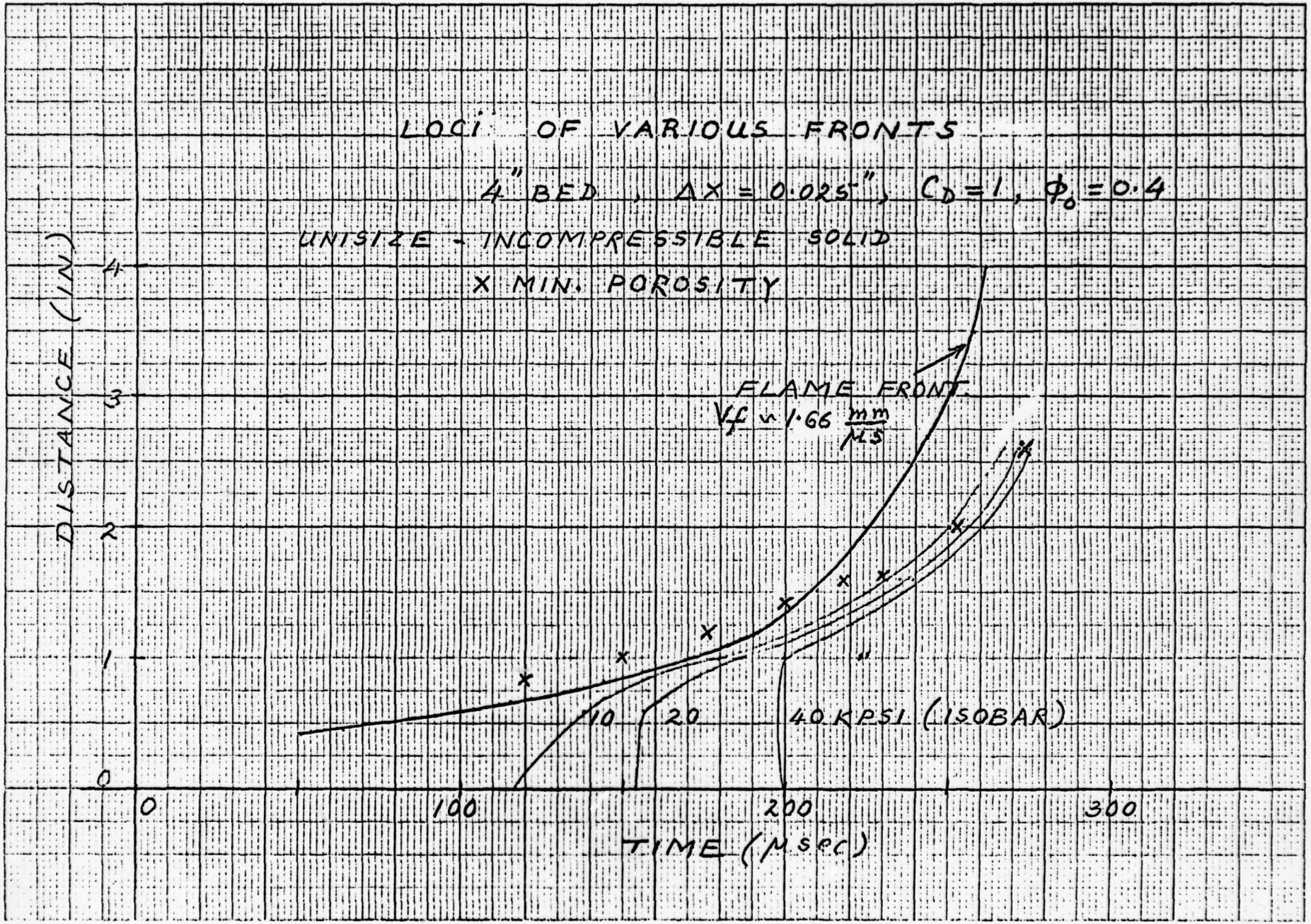

LOCI OF VARIOUS FRONTS
4" BED , ΔX = 0.025", C_D = 1, ϕ_0 = 0.4
UNISIZE - INCOMPRESSIBLE SOLID
X MIN. POROSITY
FLAME FRONT
$V_f \sim 1.66 \frac{mm}{\mu s}$
10
20
40 KPSI (ISOBAR)
DISTANCE (IN.)
TIME (μSEC)
0
1
2
3
4
100
200
300

FIGURE 6

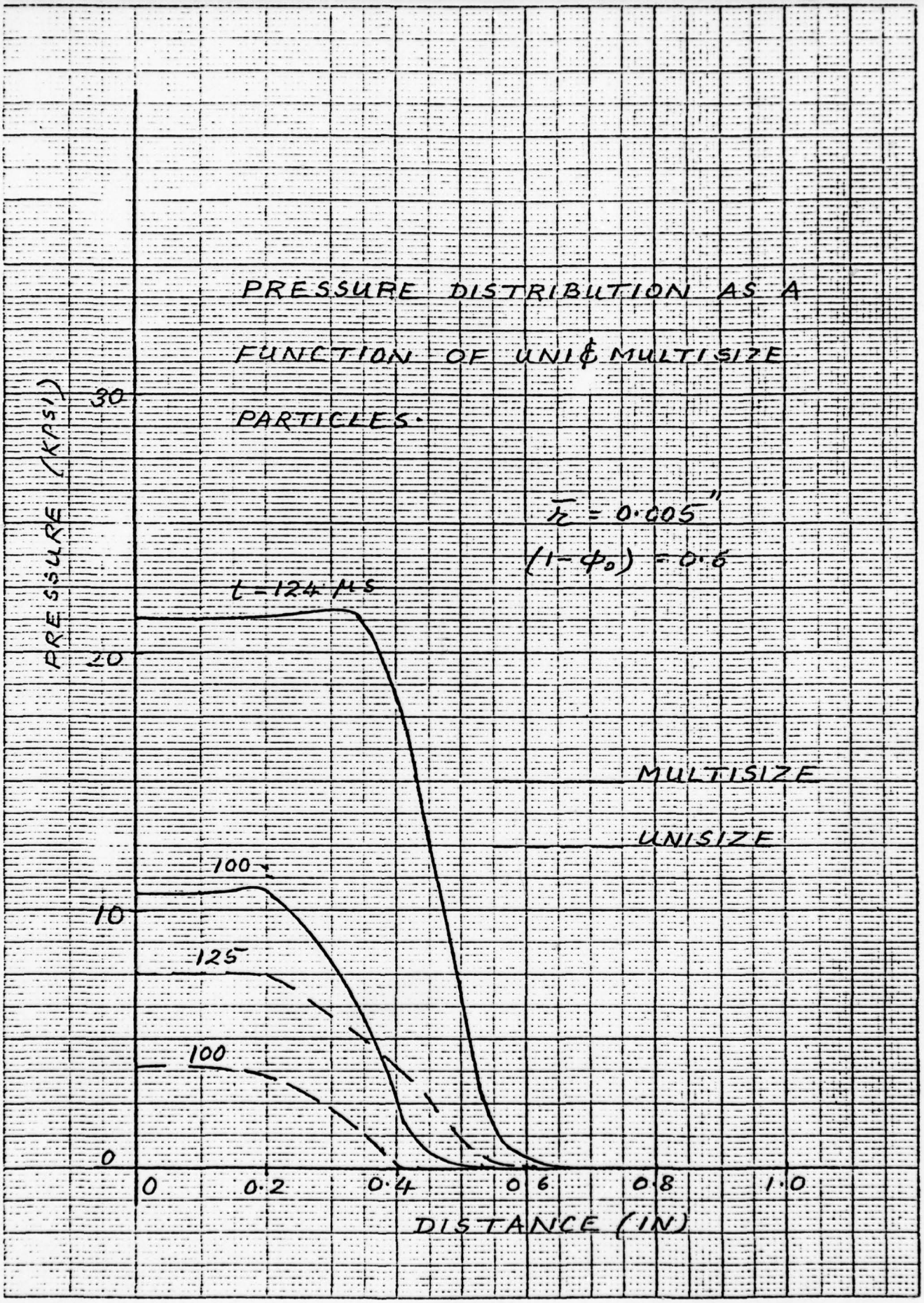

PRESSURE DISTRIBUTION AS A FUNCTION OF UNI & MULTISIZE PARTICLES.
$\bar{r}$ = 0.005"
$(1-\phi_0)$ = 0.6
t = 124 μs
PRESSURE (KPSI)
30
20
10
0
MULTISIZE
UNISIZE
100
125
100
0
0.2
0.4
0.6
0.8
1.0
DISTANCE (IN)

FIGURE 7

FIGURE 8

K+E 20 X 20 TO THE INCH • 7 X 10 INCHES
KEUFFEL & ESSER CO. MADE IN U.S.A.
46 1242

SUMMARY OF PUBLICATIONS

1. Direct Initiation of Detonation using Finite Amplitude Wave Acceleration, by John Kelvin Soldner, M.S. Thesis, Department of Aeronautical and Astronautical Engineering, University of Illinois at Urbana-Champaign (under the direction of R. A. Strehlow)(1979).

2. An Investigation in the Ignition Delay Times for Propylene Oxide - Oxygen - Nitrogen Mixtures, by Earl Edward Meister III, M.S. Thesis, Department of Aeronautical and Astronautical Engineering, University of Illinois at Urbana-Champaign (under the direction of R. A. Strehlow)(1978).

3. The Blast Wave Generated by Spherical Flames, by R. A. Strehlow, R. T. Luckritz, A. A. Adamczyk, and S. A. Shimpi, Combustion and Flame, in press, 1979.

4. Direct Detonation Initiation by Localized Enhanced Reactivity, by H. O. Barthel and R. A. Strehlow, University of Illinois at Urbana-Champaign, Paper No. 79-0286, 17th Aerospace Sciences Meeting, New Orleans, LA, January 15-17, 1979.

5. A Separate Two-Phase Flow Analysis to Study DDT in Granulated Propellant, by Herman Krier and James Kezerle, 17th Symposium (International) on Combustion, The Combustion Institute (1979, in press).

6. Modeling DDT in Granulated Reactive Solids, by S. S. Gokhale, Ph.D. Thesis, Department of Aeronautical and Astronautical Engineering, University of Illinois at Urbana-Champaign (under the direction of H. Krier), in press.

TALKS/PRESENTATIONS ON AFOSR SPONSORED WORK

A. By Roger A. Strehlow

1. Direct Detonation Initiation by Localized Enhanced Reactivity. Paper presented at the 17th Aerospace Sciences Meeting, New Orleans, January 15-17, 1979.

2. Direct Detonation Initiation by Localized Enhanced Reactivity. Progress Report presented at the AFOSR Meeting, Fort Walton Beach, Florida, January 21-24, 1979.

3. Seminar entitled "Nonideal Blast Waves", presented at the Chicago Circle Campus of the University of Illinois, February 8, 1979.

4. Seminar entitled "Nonideal Blast Waves and Flame Acceleration Processes", presented at Lawrence Livermore Laboratory, Livermore, California, June 13, 1979.

B. By Herman Krier

1. A Separated, Two-Phase Flow Analysis to Predict DDT in Propellants. Paper presented at 17th Symposium (International) on Combustion, Leeds, England August 1978.

2. DDT in Granulated Propellant: Development of a Model. Presented at AFOSR/AFRPL Contractors' Meeting, Lancaster California (March 1979).

3. Seminar entitled "Fluid Mechanics of DDT in Porous Explosives. Presented at Sandia Laboratories, Albuquerque, New Mexico, April 25, 1979.

Paper for Session A-1

SEVENTEENTH (INTERNATIONAL) SYMPOSIUM ON COMBUSTION

The University of Leeds, Leeds, England, Aug. 20-25, 1978

Entitled

A SEPARATED TWO-PHASE FLOW ANALYSIS TO STUDY DEFLAGRATION-TO-DETONATION TRANSITION (DDT) IN GRANULATED PROPELLANT*

by

Herman Krier and James A. Kezerle

Department of Aeronautical and Astronautical Engineering
University of Illinois at Urbana-Champaign, USA 61801

SUMMARY

A two-phase reactive flow model is derived and solutions are applied to the analysis of the unsteady convective heat transfer in initially packed beds of granulated solid propellant or explosives. The resulting pressure wave and flame spreading event is considered the physical process that may provide for deflagration-to-detonation transition (DDT) in such granulated beds. Discussions are included as to the appropriate constitutive laws required to complete the hydrodynamic model. The paper concludes with a brief assessment regarding both the limitations of the model and another possible DDT mechanism.

---

*Work supported by US Air Force Office of Scientific Research under Grant AFOSR 77-3115.

INTRODUCTION

The transition from combustion to detonation in condensed, but porous propellants and explosives has in recent years received attention both from analytical and experimental efforts. A large amount of the experimental work has been carried out by Soviet scientists, much of which has been documented by A. F. Belyaev *et al*. [1] and recently reviewed by H. H. Bradley and T. L. Boggs [2]. The work of R. R. Bernecker and D. Price [3,4] represents detailed and specific experimental research toward understanding deflagration-to-detonation transition (DDT) in porous explosives. These latter studies clearly indicate that the buildup to detonation represents a coupling between the pressure (shock or compression) fronts and the convectively driven flame front.

As would be expected if detonation is to follow ignition (and deflagration) it is necessary, above all, to ensure a sufficiently rapid pressure buildup. In a porous combustible system, this is achieved as a result of the penetration of the gaseous combustion products into the porous interior which leads to accelerating ignition of additional burning surfaces. Thus heat transfer by conduction is replaced by convective heat transfer. The specific mechanism to achieve DDT is yet to be fully understood, but proposed phenomenological mechanisms have been proposed by Bernecker and Price [3], by R. W. Van Dolah *et al* [5], and by Belyaev *et al* [1].

The analytical work to describe the DDT process by solving the full reactive hydrodynamic conservation equations has been underway at the Univeristy of Illinois for the past few years and is reported in Refs. 6-9. The model by H. Krier and S. S. Gokhale [8] centered upon a two-phase *continuum*

knowledge of the reaction kinetics in the solid, formation of active (hot) sites, and the appropriate equation of state for expressing the solid density in terms of the extremely high pressures and temperatures. This work does not include these stages of the transition process, but our calculations show that with a rapid transition of the convectively driven flame front, in conjunction with the interaction of the pressure fronts, one may approximately indicate conditions which might lead to detonation.

THE MODEL: FIELD BALANCE CONSERVATION EQUATIONS

The one-dimensional conservation equations for a two-phase reactive mixture have been derived by most investigators through the concept of separated flow as defined in the text by G. B. Wallis [15]. This approach considers two distinct flows, each through a separate control volume, such that the sum of the volumes represents an average mixture volume and the sums of the properties of each flow represent average mixture properties of the fluid. With this approach, separate equations for continuity, momentum, and energy are written for each phase and are solved with a state equation to describe the overall flow. Panton [16] has provided the rigorous formulation with the important assumptions required to express these field balance equations. There are, of course, many other analyses that have arrived at similar forms of the equations. The Appendix presents an outline of the method we have used to work out our conservation equations.

Assumptions

The important assumptions upon which this separated flow model is based are (1) The two phases are assumed interdispersed, but separate,

coupled only by the appropriate interaction terms; (2) Each phase is a continuum and therefore derivatives are uniquely defined; (3) The total cross sectional area is the sum of the gas and solid flow areas. (The problem is quasi-one-dimensional.); (4) Solid particles are large compared to molecules and hence do not contribute to the total pressure of the mixture; (5) When combustion of particles causes mass transfer between the phases, the solid phase always loses mass while the gas phase gains it, i.e., $\Gamma \geq 0$; (6) The diameter of a typical particle can be thought of as the average diameter of the total number of particles; (7) All gases obey the nonideal Noble-Abel equation of state with a variable co-volume; (8) Heat transfer to the particles due to conduction and radiation is neglected; (9) The density of the solid phase is constant; (10) The equations are laminar in the sense that turbulent flow due to the two-phase nature of the fluid has been averaged out. (See Panton [16] for additional discussions regarding this assumption.); (11) The gases are inviscid except for their action on the particles through the drag term; (12) The fluid properties of C_p and C_v are assumed constant, but gas viscosity and conductivity are generally known functions of temperature.

The Conservation Field Balance Equations

Some of the details in the drivation of the six field balance equations have been presented in the Appendix. In order to specifically describe the state of a two-phase fluid one needs equations to solve for the following variables: ρ_g, u_g, T_g, ϕ, u_p, and T_p. The state equations are added to the field balance equations to obtain the seven required equations. Therefore two continuity equations, two momentum equations, and two energy equations will be necessary. These equations are listed below in operator form.

Gas Continuity

$$\frac{\partial \rho_1}{\partial t} = - \rho_1 \frac{\partial u_g}{\partial x} - u_g \frac{\partial \rho_1}{\partial x} + \Gamma_g \tag{1}$$

Solid Continuity

$$\frac{\partial \rho_2}{\partial t} = - \rho_2 \frac{\partial u_p}{\partial x} - u_p \frac{\partial \rho_2}{\partial x} - \Gamma_g \tag{2}$$

Gas Momentum

$$\frac{\partial u_g}{\partial t} = - u_g \frac{\partial u_g}{\partial x} - \frac{\phi}{\rho_1} \frac{\partial P}{\partial x} + \frac{(u_g - u_p)\Gamma_g}{\rho_1} - \frac{\bar{F}}{\rho_1} \tag{3}$$

Solid Momentum

$$\frac{\partial u_p}{\partial t} = - u_p \frac{\partial u_p}{\partial x} - \frac{(1-\phi)}{\rho_2} \frac{\partial \tau_p}{\partial x} + \frac{\bar{F}}{\rho_2} \tag{4}$$

Gas Energy

$$\frac{\partial E_g}{\partial t} = - u_g \frac{\partial E_g}{\partial x} - \frac{u_g P}{\rho_1} \frac{\partial \phi}{\partial x} - \frac{\phi P}{\rho_1} \frac{\partial u_g}{\partial x}$$
$$- \frac{\Gamma_g}{\rho_1} (E_g - E_g^{chem}) + \frac{\Gamma_g}{\rho_1} \left(\frac{u_g^2}{2} - u_g u_p + \frac{u_p^2}{2} \right)$$
$$+ \frac{\bar{F}}{\rho_1} (u_g - u_p) - \frac{\bar{\Phi}}{\rho_1} \tag{5}$$

Solid Energy

$$\frac{\partial E_p}{\partial t} = - u_p \frac{\partial E_p}{\partial x} + \frac{(1-\phi) u_p}{\rho_2} \frac{\partial \tau_p}{\partial x} + \frac{\Gamma_g}{\rho_2} (E_p + E_p^{chem}) + \frac{\bar{\Phi}}{\rho_2} \tag{6a}$$

It has been duly observed that several investigators, in particular Kuo *et al.* [10,11] and Gough [12], do not write a solid phase energy balance symmetric with the gas phase energy balance, like the Eq. (6) above. Instead, these investigators have decided to simply solve the unsteady heat conduction equation for the solid particle and monitor the heat gained from

the gas in the form of convective heat transfer. In this way particle ignition can be tied to a critical surface-ignition temperature. That is, one solves for the temperature distribution within the particles.

Since, in the spirit of the one-dimensional analysis, we wish to retain only one variable to define particle internal energy, i.e., $C_{v_p} T_p$, our approach requires retention of a particle energy equation, e.g., Eq. (6a). One could alternately derive the particle energy equation by a simple energy balance on one particle, and then correct the relation to account for a $(1-\phi)$ solids fraction. In that case one gets,

Solid Energy

$$\frac{\partial E_p}{\partial t} = \frac{\Gamma_g (E_p - E_p^{chem})}{\rho_2} + \frac{\bar{\Phi}}{\rho_2} \tag{6b}$$

Note that Eq. (6b) may actually be more appropriate than Eq. (6a), since the form of Eq. (6a) implies that an acceleration of the particles decreases the particle energy, that is, the solid phase is a pseudo-fluid.

In Eqs. (1-6),

$$\rho_1 = \phi\rho_g \qquad \rho_2 = (1-\phi)\rho_p \text{ , where } \rho_p = \text{constant}$$

$$\phi = \frac{A_g}{S} \qquad (1-\phi) = \frac{A_p}{S}$$

$$E_g = C_{v_g} T_g \qquad E_p = C_{v_p} T_p$$

The subscript "g" denotes gas and "p" denotes particle. The mixture cross-sectional area is denoted by S, where $S = A_p + A_g$. Also the gas generation term for spherical particles of radius r_p is noted as $\Gamma_g = -\Gamma_p$ where,

$$\Gamma_g = \left(\frac{\hat{S}}{V}\right)_p \rho_2 \dot{r} = \frac{3}{r_p} (1-\phi)\rho_p \dot{r} \tag{7a}$$

and the propellant burning rate, $\dot{r}$, is assumed given by the relation

$$\dot{r} = b\left(\frac{T_p}{T_{p_o}}\right)^m \left(\frac{p}{P_o}\right)^n \tag{7b}$$

where b, m, and n are assumed known constant. Actually propellant burning rates at the high pressures required here have generally never been measured. Dynamic burning rates, i.e., $\dot{r} = \dot{r}(dp/dt)$ may also be important, but there are no data to take this into account.

The equation of state for the propellant gases at the expected high pressures is given by

$$P[\frac{1}{\rho} - B(\rho)] = RT \tag{8}$$

where $B(\rho)$ is variable co-volume correction based on the work of M. Cook [17].

The interphase heat-transfer $\overline{\Phi}$ represents

$$\overline{\Phi} = \frac{3}{r_p}(1-\phi)h_{pg}(T_g - T_p) \tag{9}$$

and h_{pg} = heat transfer coefficient based on Denton's work [18] through packed beds of inert particles. We therefore assume

$$h_{pg} = 0.58\frac{k_g}{r_p} Re^{0.7} Pr^{.33} \tag{10}$$

Likewise a constitutive relation is required for the interphase viscous forces, given by the term $\overline{F}$ in Eqs. (3) and (4). Here we have utilized either Ergun's drag correlation [19] or Kuo/Nydegger's relation [20]. That is

$$\overline{F} = \frac{\mu_g}{4r_p^2}(u_g - u_p) f_{pg} \tag{11a}$$

where for Ergun's data,

$$f_{pg} = \frac{(1-\phi)}{\phi^2} \{1.75\ Re + 150(1-\phi)\} \tag{11b}$$

and the Reynold number,

$$Re = \frac{2r_p \phi \rho_g |u_g - u_p|}{\mu} \tag{11c}$$

and

$$P_r = \mu_g (C_p)_g / k_g$$

It should be noted that both the coefficients h_{pg} and f_{pg} were correlated at pressures and temperatures, and thus at Reynolds numbers, several orders of magnitude less than for conditions arrived at in the DDT problem. In addition, the solid particles here, once ignited, generate gases at their surface, so that both Denton's and Ergun's correlations may only marginally apply.

Additional relations are required for the gas conductivity, k_g, gas viscosity, μ_g, and gas specific heat, C_{v_g}, as they vary with temperature and pressure, and are assumed known.

Finally, a relation is required for the resistance to compaction, at high solid loading, as symbolized by the term τ_p. Again very little data are known for the dynamic normal axial stress for an aggregate of particles, but we have used the same expression given by Kuo and Summerfield [10] have utilized. That is, beyond some critical solids load, less than $(1-\phi_c)$,

$$\tau_p = \frac{K}{1-\phi} \left\{ \frac{1}{1-\phi_c} - \frac{1}{1-\phi} \right\} \tag{12}$$

where K is a bulk modulus for the aggregate. Since for uni-sized spherical particles, minimum compaction cannot exceed 74%, the value for K must be large enough so that the normal axial stress, proportional to $\partial \tau_p / \partial x$, prevents further acceleration of the particles.

Problem of Concern

The two-phase separated flow model generates a set of six nonlinear, inhomogeneous, and coupled hyperbolic partial differential equations, as demonstrated above. The numerical method chosen for solving these equations is the explicit two-step MacCormack scheme. This method was chosen for its accuracy and because it is well documented as a two-step, predictor-corrector method of integration. Ref. 9 gives details of how we utilized this scheme, how stability was assured, and how the boundary conditions were handled at the closed ends. Equations (1-6) have also been shown to constitute a hyperbolic system of equations, as required.

Typically a bed of highly loaded, energetic small particle propellant with solids loading ranging from 0.5 to 0.7 was considered and analyzed with closed ends. Bed lengths from 5 cm to 15 cm were considered, and the space domain divided in grids of $\Delta x = 0.1$ cm. Stability, dependent upon the gas velocities and mixture sound speed required that the time increment, Δt, be of the order of 0.5 useconds.

The problem was initialized by assuming that at time, $t = 0$, a pressure pulse, typically 10 M N/m^2 (1500 psi) was distributed over the first 10 percent of the bed. It was also assumed that near one end 3% of the bed was initially ignited, that is $T_p > T_{p(ign)}$. The ignition criteria employed here requires that if the particle energy $E_p \geq E_{p(ign)}$, an assumed known value, they begin to burn, at a rate given by $\dot{r}_p$. Thus, $T_{p(ign)} \equiv E_p(ign)/C_{v_p}$.

After several hundred independent calculations a baseline case with standard input conditions was deduced. It should be noted that the solid phase stress tensor in Eq. (4) does not include the gas pressure. The reason for this is that it has been shown [8] that the set of equations will be

totally hyperbolic only if there is no gas pressure gradient in the solid phase momentum equation.

Table 1 summarizes the most important input used to carry out the typical results shown below. The main results presented from this analysis are the pressure distributions as time progresses, the flame front locus and pressure front(s), as well as developments in the temperature and velocity fields.

Results from the Baseline Case

Figures 1 through 5 present the distribution histories of the fluid dynamic variables in a bed of solid propellant 7.56 cm (3 in.) long, with a solids loading at 60 percent (ϕ_o = 0.40). The results in these figures were termed the baseline case, as defined above.

Figure 1 outlines the calculated pressure distributions at four different times. As in previous work related to this problem (see Ref. 8) the appearance of a "continental-divide" in the interior of the bed is pronounced and pressure gradients are extremely steep. In addition, the average pressures behind the front are very high, reaching in excess of 3.4 G N/m^2 (0.5 x 10^6 psia). Such pressures may be unrealistically high when compared to experiments in closed pipes as reported in Refs. 3 and 4, due to the fact that here we are assuming incompressible solid particles, all spherical in shape, so that once ignited all surfaces generate gases. Irregular shaped, compressible particles may compact in such a way to prevent all available surfaces from burning, even though the solid temperatures are beyond the critical ignition temperature.

The locus of the flame (ignition) front for the baseline case is presented in Fig. 2, where the deflagration speed (slope of the x-t locus)

accelerates to several mm/μs. Also shown in this figure is a line labeled the "pressure front." This locus was derived by noting the midpoint of the pressure wave shown in Fig. 1 at various times. It appears that the pressure front and the flame front are coincident as the

Table 1

TYPICAL INPUT DATA

Parameter	Value
Initial bed temperature, T_g, T_p	294.0°K
Bulk itnition temperature, T_{ign}	314°K
Range of initial bed porosity, ϕ	0.30 - 0.50
Propellant burning rate proportionality constant, b	1.24 cm/s $(MPa)^n$
Propellant burning rate index, n and m	0.90 and 0.25
Propellant density, ρ_p	1.58 g/cm^3
Initial grain diameter, $d_p = (2r_p)$	400 μm
Chemical energy released, $E_{chem} = (E_g - E_p)^{chem}$	5.48 MJ/kg
Latent heat of propellant sublimation $(E_p{}^{chem})$	0.22 MJ/kg
Molecular weight of gas, MW	22.6 kg/kg-mole
Covolume of propellant gas, B_v (at moderate pressures)	1.08 cm^3/g
Specific heat ratio of gas, γ	1.252
Gas viscosity, μg (at 2000 K)	4.45 N-s/m^2
Gas specific heat at constant volume (2000 K)C_{v_g}	0.340 cal/gram °K
Solid specific heat at constant volume, C_{v_p}	0.305 cal/gram °K
Total bed length, L_B	75.0 mm
Bulk modulus, K (Eq. 12)	48 M N/m^2
Compaction initiation porosity, ϕ_c (Eq. 12)	0.42

flame accelerates to complete ignition.

Figure 3 shows both the gas velocity and the propellant particle velocity distributions at the chosen times. As might be expected, the velocity peaks shown are a consequence of the steep pressure front arriving at the various locations. Also worth noting are the extreme gas velocities, often exceeding 1500 m/s, and the fact that peaks in particle velocity lag peaks in gas velocity at any given time.

Figure 4 presents gas temperature and particle temperature distribution histories. With the chemical energy fixed for this propellant, the gas temperatures are generated at values of roughly 3600°K. These temperatures decay as the gases lose heat to the solid by convection into the bed interior. Later, as the pressure front steepens, the gases are compressed in the interior to values far exceeding their incoming values. The subsequent particle temperatures are increased not only due to the convective heat transfer, but also due to the rapid changes in kinetic energy of these mobile particles.* The last predictions displayed for the baseline case are the porosity distribution histories shown in Fig. 5. The porosity profiles show that near the front of the bed (which is partially ignited at t = 0) the porosity increases fairly rapidly. This is due to both a reduction in volume of the particles due to burning and the forward motion of these particles being dragged along by the gases. Subsequent to this, the particles are compacted somewhere in the bed interior to solids loadings greater than the original 60 percent. (Recall that the solid fraction equals $(1-\phi)$.) Also, for the results shown here a significant fraction of the bed has been consumed (due to rapid burning at the high pressures) at times in excess of 50 μs.

Decreasing the particle size from the 200 μm diameter (r_p = .004 inches)

*With Eq. (6b) used instead of Eq. (6a), particle energies are latered only by convective heat transfer to the particle surface.

yields a trend similar to increasing the solids loading. In the case shown in Fig. 6, decreasing the radius to 100 μm results in an increase in the $(\hat{S}/V)_p$ ratio of the particles of 100 percent, since $(\hat{S}_p/V_m)_o = 3(1-\phi_o)/r_p$. For the input data base used here, the predicted pressures for the small particles size exceeded $7\cdot(10^9)$ N/m^2. Therefore the maximum pressure in the bed as a function of particle size, as presented in the insert, is shown for an arbitrary time of 26.6 μs, and not when the whole bed was ignited.

An alternate pressure wave "front" can be defined by first plotting pressure vs. time at any of the downstream x-locations in the bed, and this is shown in Fig. 7 for a case using a slightly different form of the particle energy equation, i.e., Eq. (6b). The locus of a pressure front can then alternately be defined as the time at any position when the pressure begins its rapid increase. For example, on Fig. 7, at x = 3.8 cm, the pressure front is said to arrive at 82 μs. This locus is plotted along with the ignition (flame) front on Fig. 8. Notice the fairly abrupt change in flame (deflagration) speed at approximately 60 μs, which approximately coincides with the intersection of the pressure front as obtained from Fig. 7: The calculations of the flame front, pressure wave front shown in Fig. 8 have many of the same features as those observed in the DDT tests reported by Bernecker and Price [3]. Although the predictions shown here cannot yet be termed actual DDT, they do represent indications of the rapid propellant combustion, producing high pressures which drive hot product gases into the unignited pores in a rapidly accelerating fashion. When calculations of the type shown in the previous figures were repeated for low-to-medium energy content solid propellant, say 750 cal/g, no such dynamic acceleration (as shown in Fig. 8) were predicted, even in bed lengths twice the nominal value

of 7.5 cm. Similarly flame speeds with the high-energy propellant (see Table 1), but with a burning rate constant, b, one-half of the nominal baseline value, never accelerated beyond 0.2 mm/μs in the bed lengths studied here.

CONCLUDING REMARKS

Using the concept of a separated-flow two-phase mixture of solid propellant particles and their resulting gaseous products, the one-dimensional form of the appropriate governing conservation relations were solved along with a series of constitutive relations. It was mentioned that many of these latter relations were utilized for conditions in this problem which are well removed from those as they were originally obtained. The report by Krier and Kezerle [9] presents various sensitivity studies in which the interphase heat transfer and drag correlations were altered, and where the ignition energy was varied. The conclusions derived from such a study were that, on the whole, the results shown here represent the general behavior of the flow variables during the dynamic flame-spreading process. This does not mean that one is necessarily satisfied with the accuracy of these constitutive laws. But rather, if precise predictions for DDT are to be reported, additional two-phase experiments (at high pressures and high gas temperatures) will first be required.

The key conclusions from this study are then,

(1) On the average, the convective mode combustion dynamics through granulated propellant is the same using either the separated flow concept or the continuum mixture concept of Ref. 8, although in this paper we have not presented such comparisons.

(2) As would be expected, only highly energetic, rapid burning rate

propellants exhibit the acceleration to detonation-like flame and pressure fronts.

(3) Quantitative predictions for the run-up distances to detonation may have to be delayed until better information is available for the gas-particle forces and heat transfer, for the particle-particle forces, and for the solid ignition criteria for these transient flow processes.

(4) However, with pressures in the granulated bed, typically predicted to exceen 20 Kbar (2 G N/m^2), in time periods under 50 μs, one may begin to consider DDT phenomena of the condensed phase alone, due to classical shock initiation. This aspect was not considered in this study. If this were a possibility, one might consider the existence of an alternative hazard potential for solid propellants or explosives, in which a portion of the solid first sustains damage in which cracks formed which were partially filled with small granulated particles. If such a particle laden fissure finds a source of ignition, then the convective mode combustion of these small particles under confinement can generate an accelerating flame and the subsequent high "shock" pressures to detonate the compacted consolidated solid particles in the crack. In order to analyze such a shock hydrodynamic condition one would couple the solution of the granular bed flame spreading with the dynamic deformation of the compacted solid. An equation of state would be required for the solid density, ρ_p, as a function of the pressure and temperature. Then a shock analysis of transition to detonation would follow, as, for example, by the formalism outlined by Forest [22].

References

1. Belyaev, A. F. et al.: *Transition from Deflagration to Detonation in Condensed Phases*, Institute of Chemical Physics; available as TT 74-50028, National Tech. Inf. Service, 1975.
2. Bradley, H. H. and Boggs, T. L.: *Convective Burning in Propellant Defects -- A Literature Review*, Naval Weapons Center, Report NWC TP-6007, 1978.
3. Bernecker, R. R. and Price, D.: Combustion and Flame 22, 111-129, 161-170, 1974.
4. Price, D. and Bernecker, R. R.: *DDT Behavior of Ground Tetryl and Picric Acid*, Naval Surface Weapons Center, Report NSWVC/WOL TR 77-175, 1978.
5. Van Dolah, R. W. et al.: *Explosion Hazards of Ammonia Nitrate under Fire Exposure*, Bureay of Mines, Report 6773, 1966.
6. Krier, H., *Two-Phase Transport and Reactor Safety*, Vol. 1, (T. N. Veziroglu, S. Kakac, Eds.), pp. 363-383, 1976.
7. Van Tassell, W. F. and Krier, H.: Int'l. J. Heat & Mass Transfer 18, 1377-86, 1975.
8. Krier, H. and Gokhale, S. S.: AIAA J. 16, 177-183, 1978.
9. Krier, H. and Kezerle, J. A.: *Modeling of Convective Mode Combustion through Granulated Propellant to Predict DDT*, University of Illinois at Urbana-Champaign, Report UILU-Eng 77-0517; also available as AFOSR TR 78-007, 1977.
10. Kuo, K. K. and Summerfield, M.: *Fifteenth Symposium (International) on Combustion*, pp. 515-525, The Combustion Institute, 1974.

11. Kuo, K. K. et al.: Acta Astronautica 3, 573-591, 1976.

12. Gough, P.: *Fundamental Investigation of the Interior Ballistics of Guns*, Space Corporation, Report SRC-R-74, 1974.

13. Crowe, C. T.: *Proceedings of the 1976 Heat Transfer and Fluid Mechanics Institute*, pp. 214-227, Stanford University Press, 1976.

14. Hughes, E. D.: *Two-Phase Transport and Reactor Safety*, Vol. 1 (T. N. Veziroglu and S. Kakac, Eds.), pp. 407-453, 1976.

15. Wallis, G. B.: *One-Dimensional Two-Phase Flow*, McGraw-Hill Book Co., New York, NY, 1969.

16. Panton, R.: J. Fluid Mechanics 31, 273-303, 1968.

17. Cook, M. S.: *The Science of High Explosives*, American Chemical Society Monograph Series, Reinhold Publ. Corp., New York, NY, 1963.

18. Denton, W. H.: Institute of Mechanical Engineers J. (and ASME) 2, 370, 1951.

19. Ergun, S.: Chemical Engineering Progress 48, 89-96, 1952.

20. Kuo, K. K. and Nydegger, C. C.: J. of Ballistics 2, 1-26, 1978.

21. Green, A. E. and Naghdi, P. M.: Quarterly J. Mechanical and Applied Math. 22, part 4, pp. 427-438, 1969.

22. Forest, C. A., *Burning and Detonation*, Los Alamos Scientific Lab., University of California; Report LA-7245 (1978).

APPENDIX

Some Details of the Derivation of the Field-Balance Conservation Equations for Two-Phase Separated Flow

There are many ways to derive the quasi-one-dimensional continuity, momentum, and energy equations for the gas and particle phase. The work of Panton [16] is a good example of a rigorously mathematical approach. An alternative but closely related derivation is shown below in which the gas phase and solid phase are treated separately, in their own control volumes, such that the sum of these volumes adds to the mixture volume. But each phase is treated as a continuum, so that when the solid-phase is analyzed it is treated as a "fluid" of properties ρ_p, u_p, and T_p.

Conservation of Mass:

For the gas phase one begins by expressing gas-continuity as

$$\frac{\partial(\rho_g A_g)}{\partial t} = -\frac{\partial(\rho_g u_g A_g)}{\partial x} + \Gamma_c S \qquad \text{(A-1)}$$

where $A_g = \phi S$ and S is the total cross-sectional area of the (mixture) control volume. Defining $\rho_1 = \phi\rho_g$, one gets

$$\frac{\partial \rho_1}{\partial t} + \frac{1}{S}\left[\rho_1 u_g \frac{\partial S}{\partial x} + \rho_1 S \frac{\partial u_g}{\partial x} + u_g S \frac{\partial \rho_1}{\partial x}\right] = \Gamma_c \qquad \text{(A-2)}$$

The particle phase is treated in a similar manner, except u_p replaces u_g, A_g is replaced by A_p, where $A_p = (1-\phi)S$ and $\Gamma_{c_p} = -\Gamma_c$. Here Γ_c is the gas source term due to pyrolysis of the solid particles. One arrives at

$$\frac{\partial \rho_2}{\partial t} + \frac{1}{S}\left[\rho_2 u_p \frac{\partial S}{\partial x} + \rho_2 S \frac{\partial u_p}{\partial x} + u_p S \frac{\partial \rho_2}{\partial x}\right] = -\Gamma_c \qquad \text{(A-3)}$$

where $\rho_2 = (1-\phi)\rho_p$.

Conservation of Momentum

For the gas phase one simply expresses the time rate of increase of momentum inside the control volume to be equal to the sum of all forces acting on the control surfaces. Thus,

$$\frac{\partial(\rho_g A_g u_g)}{\partial t} = -\frac{\partial(\rho_g A_g u_g^2)}{\partial x} + \Gamma_c u_p S - A_g \frac{\partial P}{\partial x} - \bar{F}S \qquad \text{(A-4)}$$

Note that it is assumed the pressure gradient force acts only on the area A_g. It is also assumed that since the gas is formed at a velocity equal to the particle velocity, there is a source of gas momentum per unit area equal to $\Gamma_c u_p$. Of course the solid phase must have a sink of momentum equal to that amount. Also, here, $\bar{F}$ represents the viscous interaction forces between the gas and all the solid particles.

To express (A-4) in operator form, one again introduces the variable ϕ, then multiplies Eq. (A-2) by u_g, then subtracts that equation from (A-4) to get

$$\rho_1 \frac{\partial u_g}{\partial t} + \rho_1 u_g \frac{\partial u_g}{\partial x} = \Gamma_c(u_p - u_g) - \phi \frac{\partial P}{\partial x} - \bar{F} \qquad \text{(A-5)}$$

For the solid phase one begins with the momentum balance similar in form to Eq. (A-4), i.e.,

$$\frac{\partial[\rho_p(1-\phi)Su_p]}{\partial t} - \frac{\partial[\rho_p(1-\phi)Su_p^2]}{\partial x} - \Gamma_c u_p S - (1-\phi)S\frac{\partial \tau_p}{\partial x} + \bar{F}S \qquad \text{(A-6)}$$

Again using the Eq. (A-3), first multiplied by u_p and substituting into (A-6) one arrives at

$$\rho_2 \frac{\partial u_p}{\partial t} + \rho_2 u_p \frac{\partial u_p}{\partial x} = -(1-\phi) \frac{\partial \tau_p}{\partial x} + \overline{F} \qquad \text{(A-7)}$$

where we assume ρ_p = constant, and where τ_p represents the normal-axial compressive stress (see Eq. 12).

Conservation of Energy

For the gas phase, the first law of thermodynamics for a control volume provides that

$$\rho_g A_g q_e = F u_p S + \overline{\Phi} S + \frac{\partial}{\partial t} [\rho_g A_g (E_g + u_g^2/2)] + \frac{\partial}{\partial x}\left[\rho_g A_g \left(E_g + \frac{u_g^2}{2} + \frac{P_g}{\rho_g}\right) u_g\right]$$

$$- \Gamma_c S \left[E_g^{chem} + \frac{u_p^2}{2}\right] \qquad \text{(A-8)}$$

where

$E_g = \int c_v dT$

$q_e = \frac{\partial}{\partial x}\left(-k \frac{\partial T}{\partial x}\right)$ (heat conduction) (neglected later)

E_g^{chem} = heat of combustion

$\Gamma_c S \frac{u_p^2}{2}$ = kinetic energy added because gases are generated with the velocity u_p.

$\overline{\Phi}$ = interphase energy transfer from gas to particles and interphase dissipation work

$= \dot{q}_{pg} + \frac{\partial}{\partial x}(\tau_{xx} u_g \phi)$, where the gas-shear stress τ_{xx} is neglected later

and where

$\dot{q}_{pg} = h_{pg}(T_g - T_p)\phi(\hat{S}_p/V_m)$ where $(\hat{S}_p/V_m) = 3(1-\phi)/r_p$.

To arrange Eq. (A-8) in operator form, one subtracts from it the product of $(E_g + u_g^2/2)$ times the continuity Eq. (A-2), and the product of (u_g) times

the momentum Eq. (A-5) to get

$$\frac{\partial E_g}{\partial t} = - u_g \frac{\partial E_g}{\partial x} - \frac{P_g}{\rho_g}\frac{\partial u_g}{\partial x} - \frac{u_g P_g}{S\rho_g}\frac{\partial S}{\partial x} - \frac{u_g P_g}{\rho_1}\frac{\partial \phi}{\partial x} + \frac{F(u_g - u_p)}{\rho_1}$$

$$- \frac{h_{pg}(T_g - T_s)\phi}{\rho_1}\left[\frac{\hat{S}_p}{V_m}\right] + \frac{\Gamma_c}{\rho_1}\left(E_g^{chem} - \frac{u_p^2}{2}\right) - \frac{\Gamma_c}{\rho_1}\left(E_g - \frac{u_g^2}{2} + u_g u_p\right) \qquad \text{(A-9)}$$

The solid phase energy equation is expressed in a similar form to Eq. (A-8), i.e.,

$$\rho_p(1-\phi)\dot{q}_p = - Fu_p - \bar{\Phi} + \frac{\partial}{\partial t}\left[\rho_p(1-\phi)(E_p + u_p^2/2)\right]$$

$$- \frac{1}{S}\frac{\partial}{\partial x}\left[\rho_p(1-\phi)Su_p\left(E_p + \frac{u_p^2}{2} + \frac{P_g}{\rho_p}\right)\right] - \Gamma_c\left[E_p^{chem} - \frac{u_p^2}{2}\right] \qquad \text{(A-10)}$$

Note the signs on the terms Fu_pS and ΦS are opposite those in the gas phase energy equation because the overall mixture equation (gas + solid) cannot have such source terms. Generally (as shown above), one would have to define $H_p = E_p + P_g/\rho_p$, that is, the solid-phase density, ρ_p and the gas-phase pressure, P_g is employed. Since the particles are incompressible, we now drop the term P_g/ρ_p in the next-to-the-last term of Eq. (A-10).

To simplify Eq. (A-10), one again multiplies the solid-phase continuity Eq. (A-3) by $(E_p + u_p^2/2)$ and multiplies the solid-phase momentum Eq. (A-7) by u_p. Both of these latter two equations are subtracted from Eq. (A-10), and assuming $\dot{q}_p$ (external heating) is neglected, one arrives at

$$\frac{\partial E_p}{\partial t} = - u_p \frac{\partial E_p}{\partial x} + \frac{(1-\phi)u_p}{\rho_2}\frac{\partial \tau_p}{\partial x} + \frac{\Gamma_c}{\rho_2}\left[E_p + E_p^{chem}\right] + \frac{\bar{\Phi}_p}{\rho_2} \qquad \text{(A-11)}$$

Here E_p^{chem} represents the latent heat of pyrolsis for the solid.

CAPTIONS: Figures 1 - 8

Figure 1. Pressure distribution during flamespreading in an initially packed bed of small particles of solid propellant. (Figs. 2-5 show variation in other flow parameters for the same case as calculated for Fig. 1.)

Figure 2. Locus of ignition (flame) front and pressure front, the latter derived from P vs x distribution.

Figure 3. Gas and particle velocity distribution history.

Figure 4. Gas and particle temperature distribution history.

Figure 5. Porosity (gas volume fraction) distribution history. The (*) indicates the location of the ignition front.

Figure 6. Ignition (flame) front locus for three different initial spherical particle sizes. The insert shows at one (arbitrary) time the peak pressure in the bed as a function of the initial size.

Figure 7. The pressure-time variation at six different locations in the bed; Eq. (6b) replaces Eq. (6a).

Figure 8. Locus of ignition (flame) front and the pressure front (derived from observations of P(t) shown in Fig. 7) indicating rapid flamespreading accerelation which may lead to DDT.

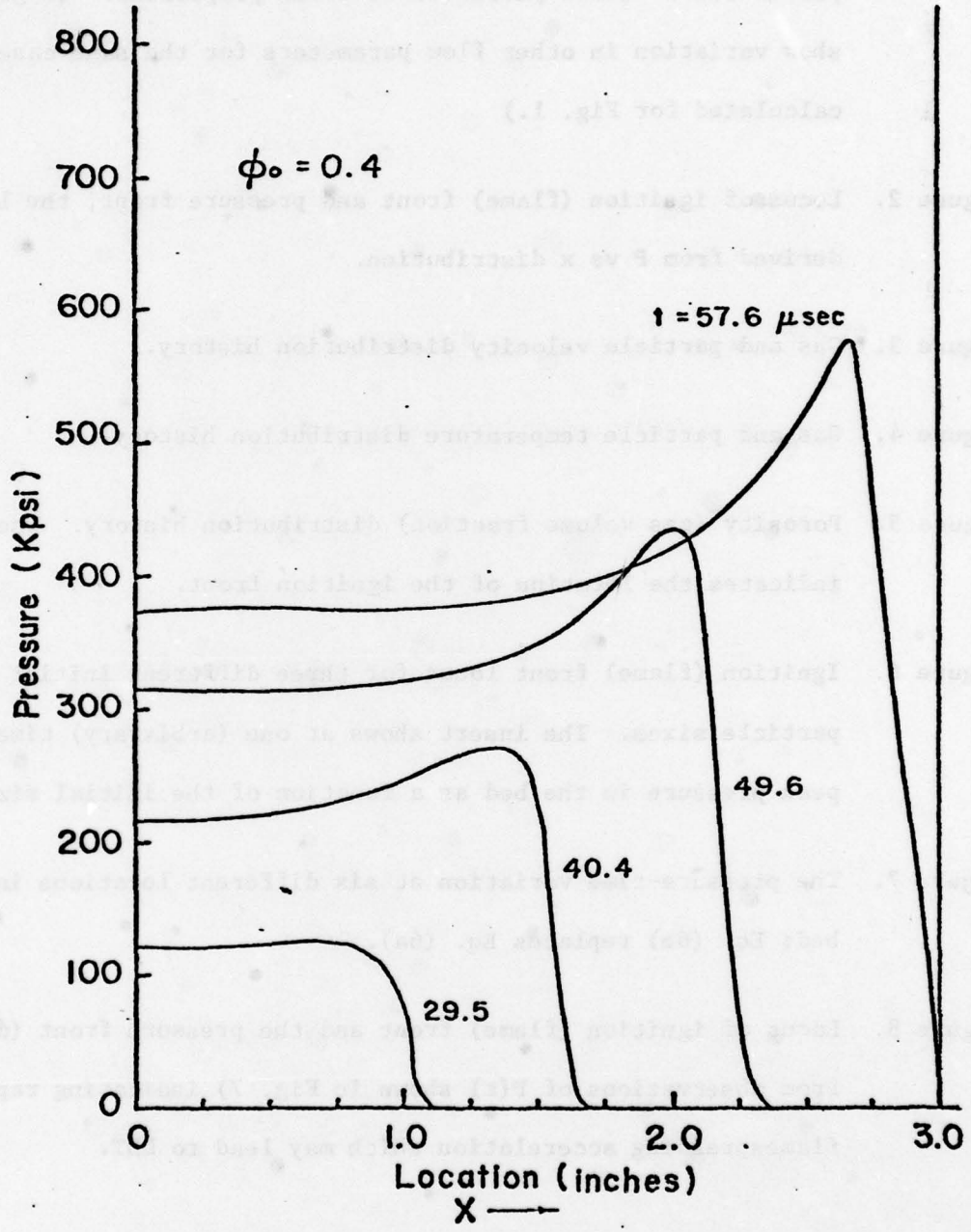


Figure 1 Pressure distribution history predicted for a three inch long bed with an initial solids loading of 60 percent. [Predictions for Figs. 1 - 5 utilized the second-form of the particle energy equation.]

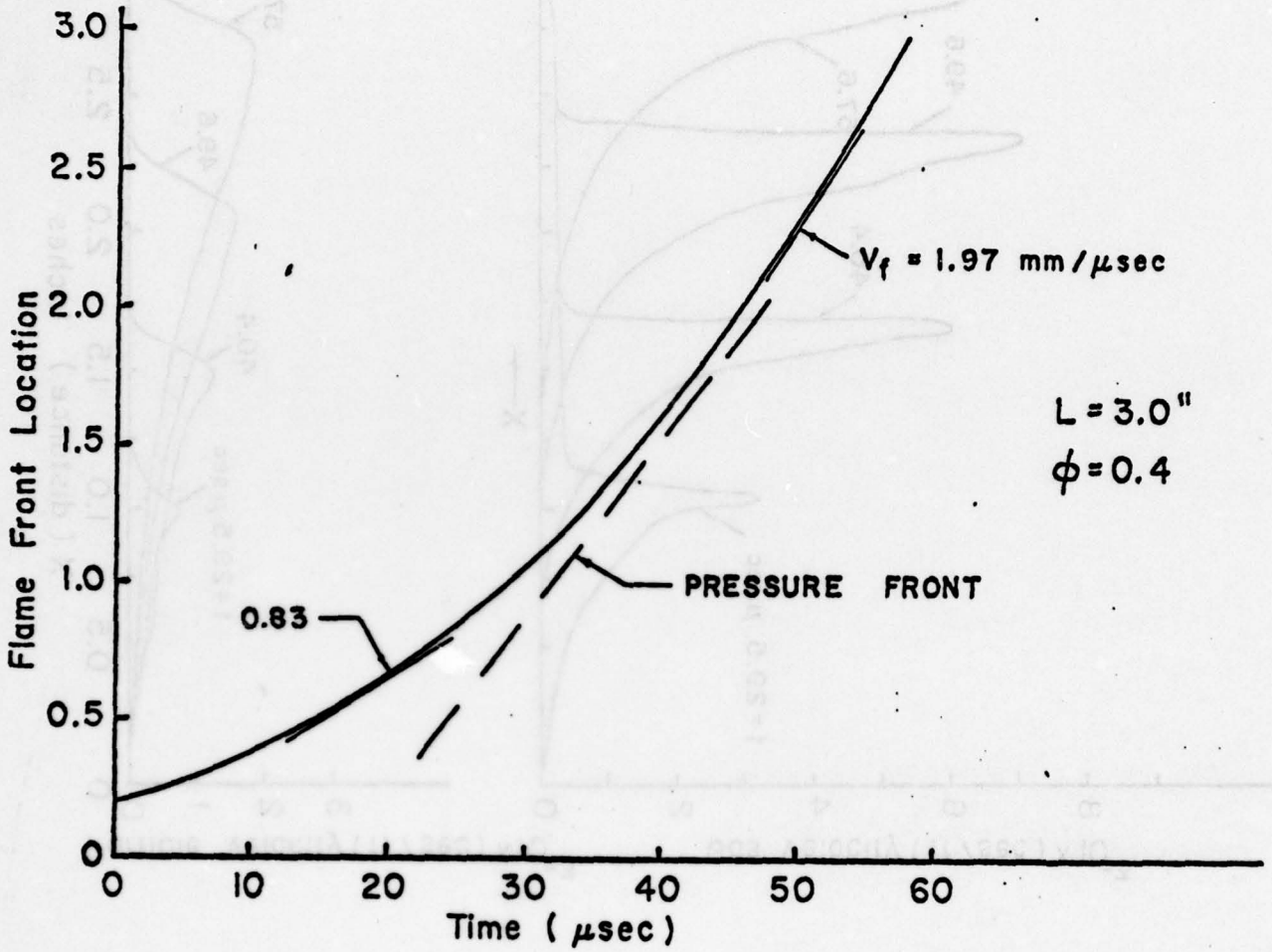


Figure 2 Flame front and pressure front loci for the pressure distributions indicated in Fig. 1.

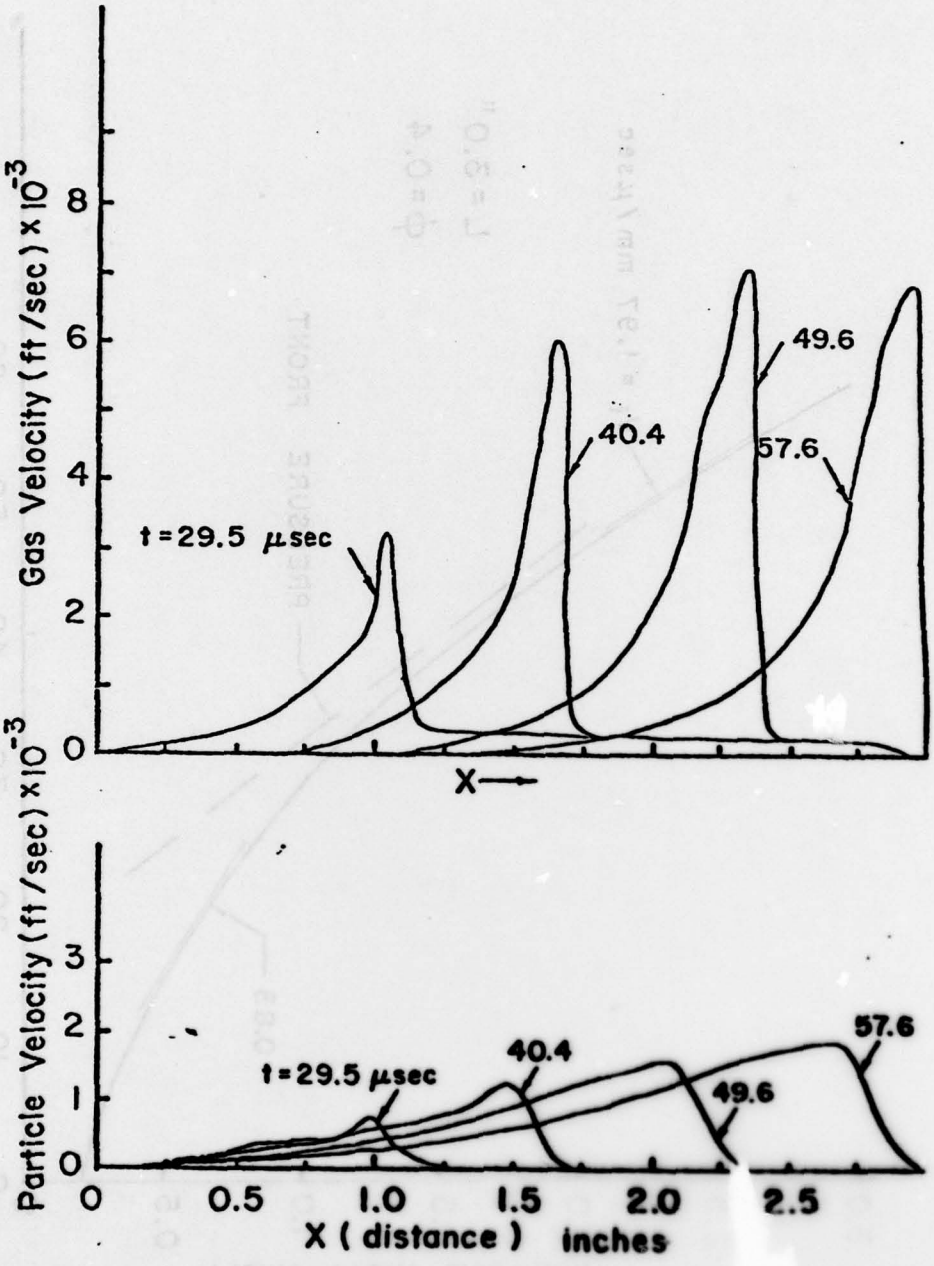


Figure 3 Gas velocity and particle velocity distribution history.

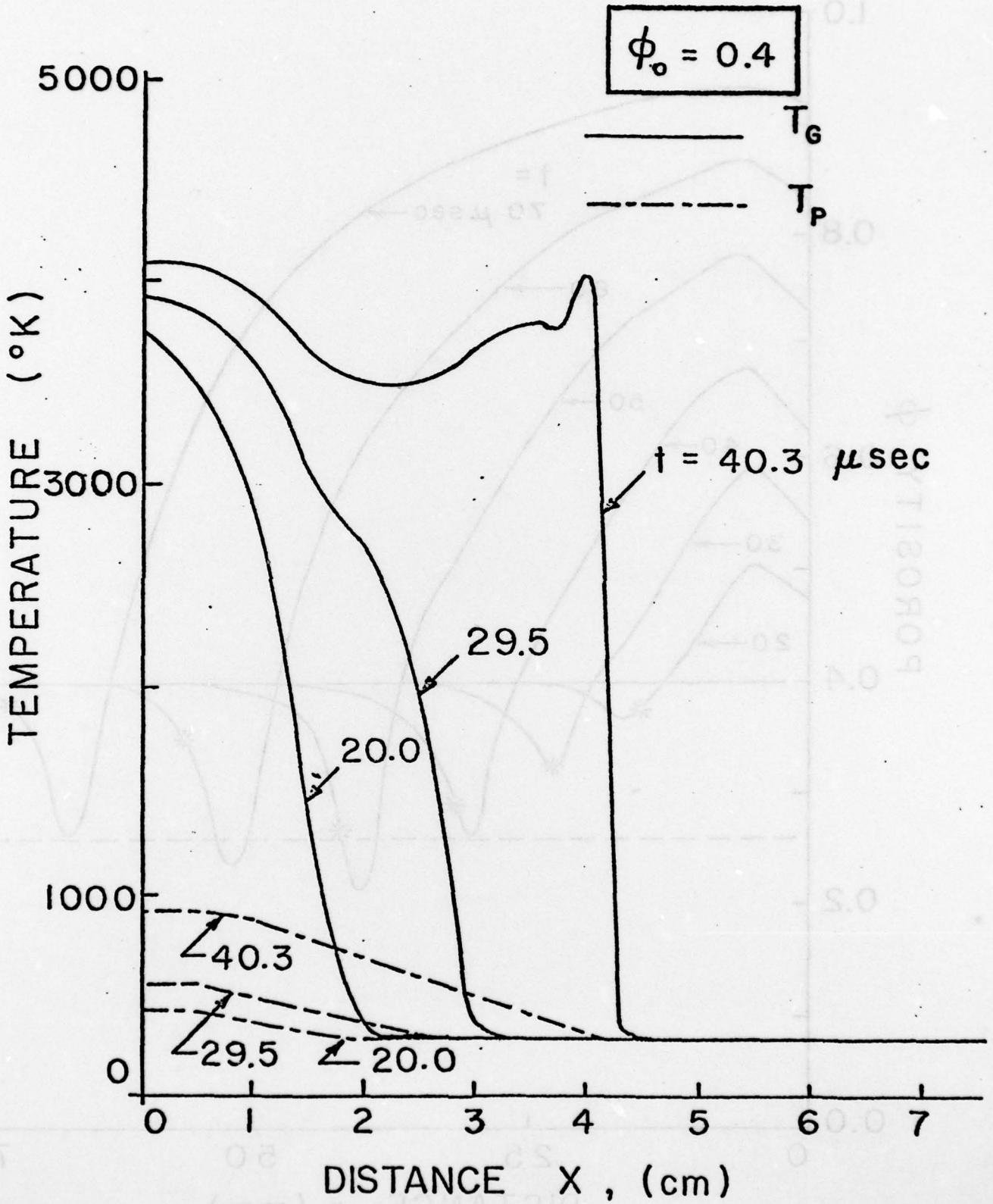
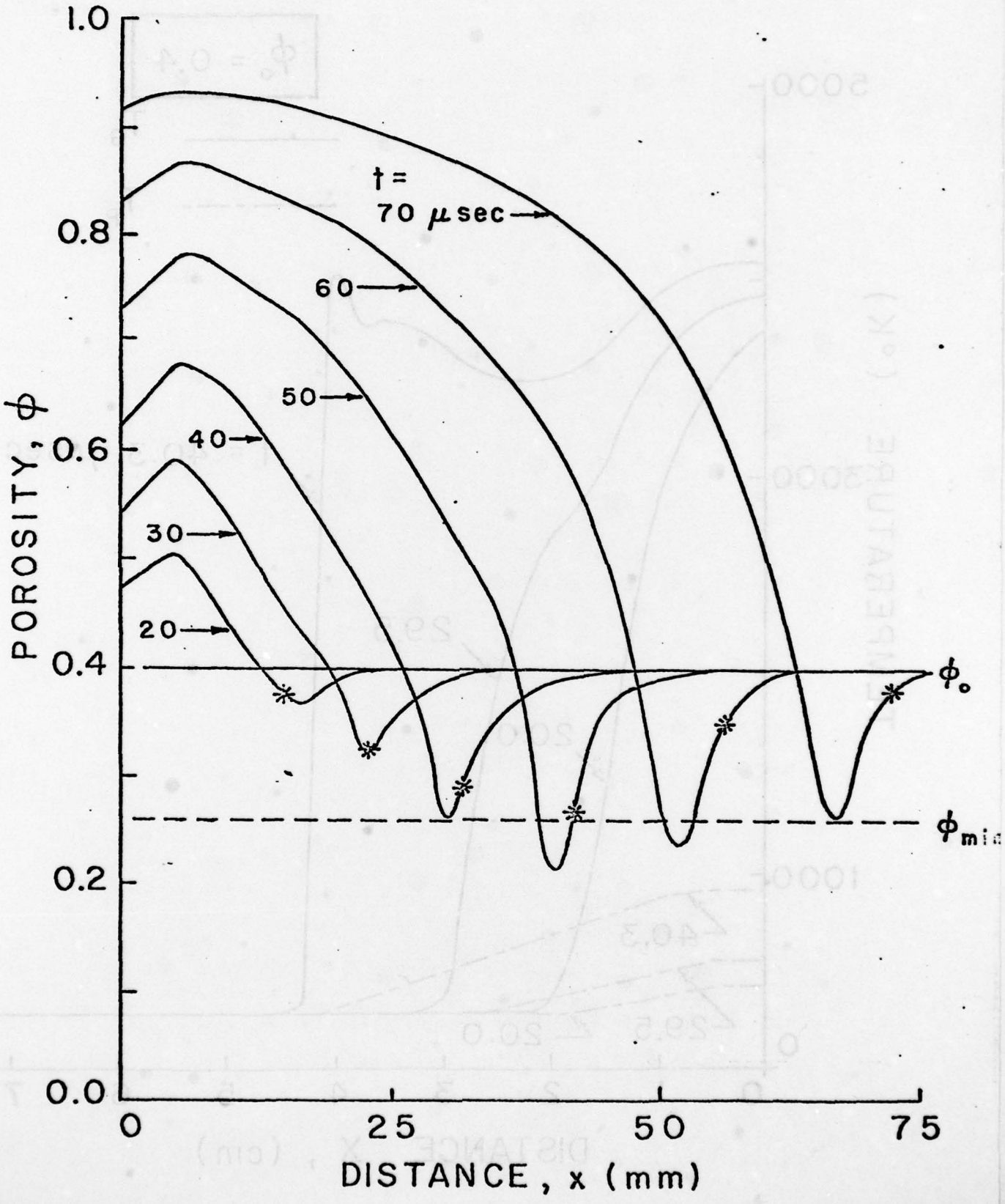

ϕ_o = 0.4
T_G
T_P
5000
3000
1000
0
TEMPERATURE (°K)
t = 40.3 μsec
29.5
20.0
40.3
29.5
20.0
0
1
2
3
4
5
6
7
DISTANCE X , (cm)

FIGURE 5


1.0
0.8
0.6
0.4
0.2
0.0
POROSITY, φ
t =
70 μsec
60
50
40
30
20
φ₀
φmin
0
25
50
75
DISTANCE, x (mm)

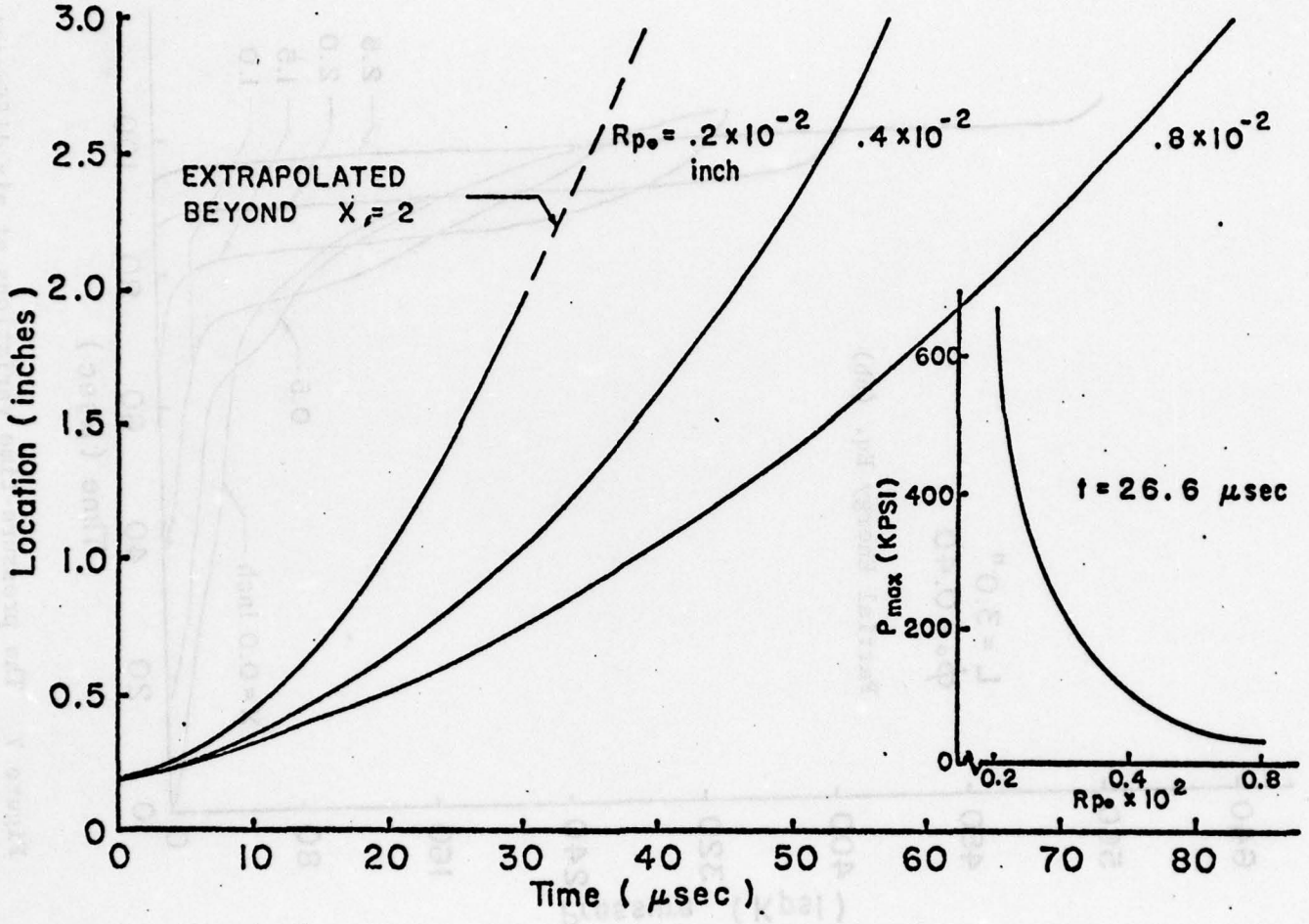


Figure 6 Flame front locus for three different initial particle sizes. [Note, R_p = 0.004 corresponds to a 200 μm diameter spherical particles.]

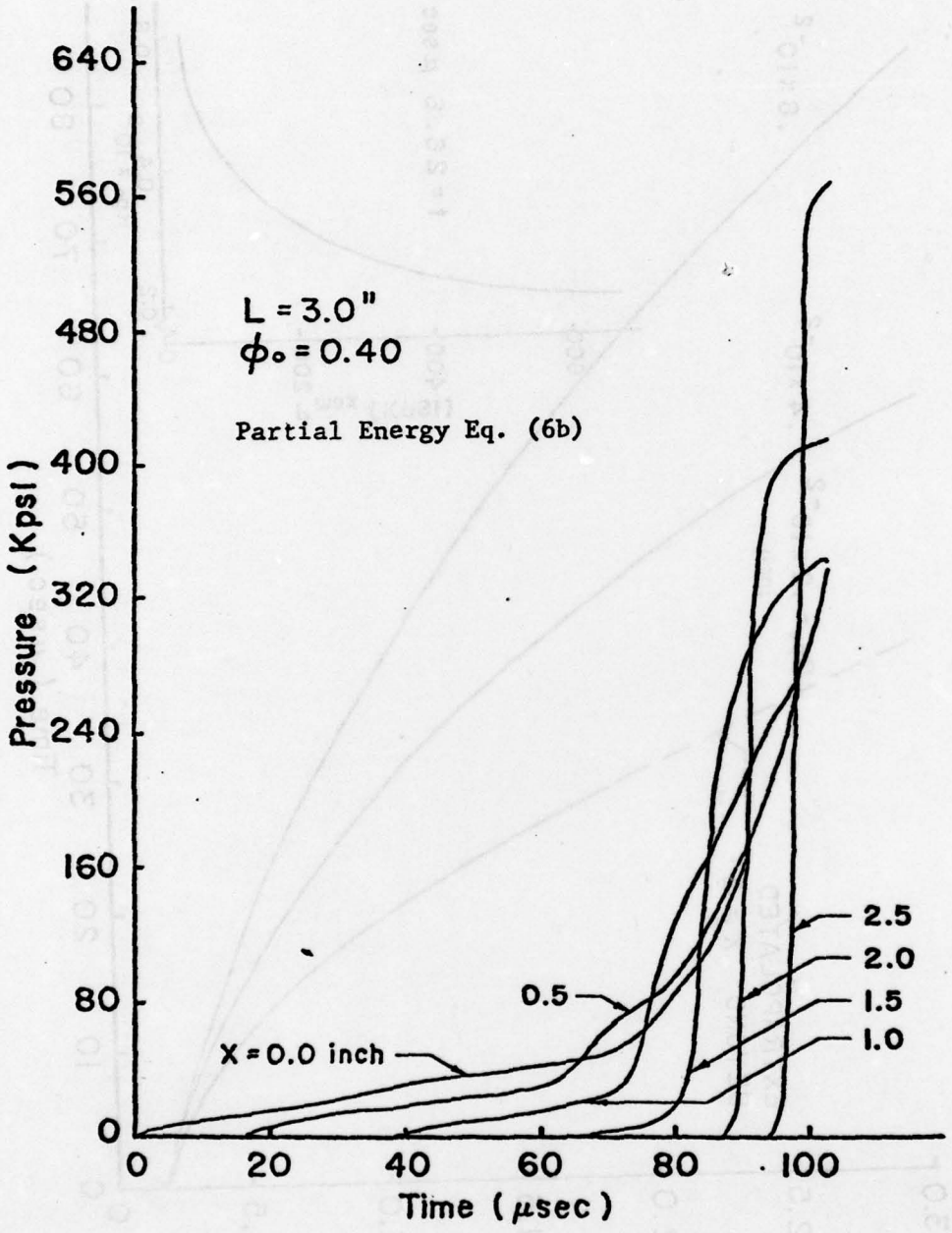


Figure 7 The pressure-time variations at six different locations.

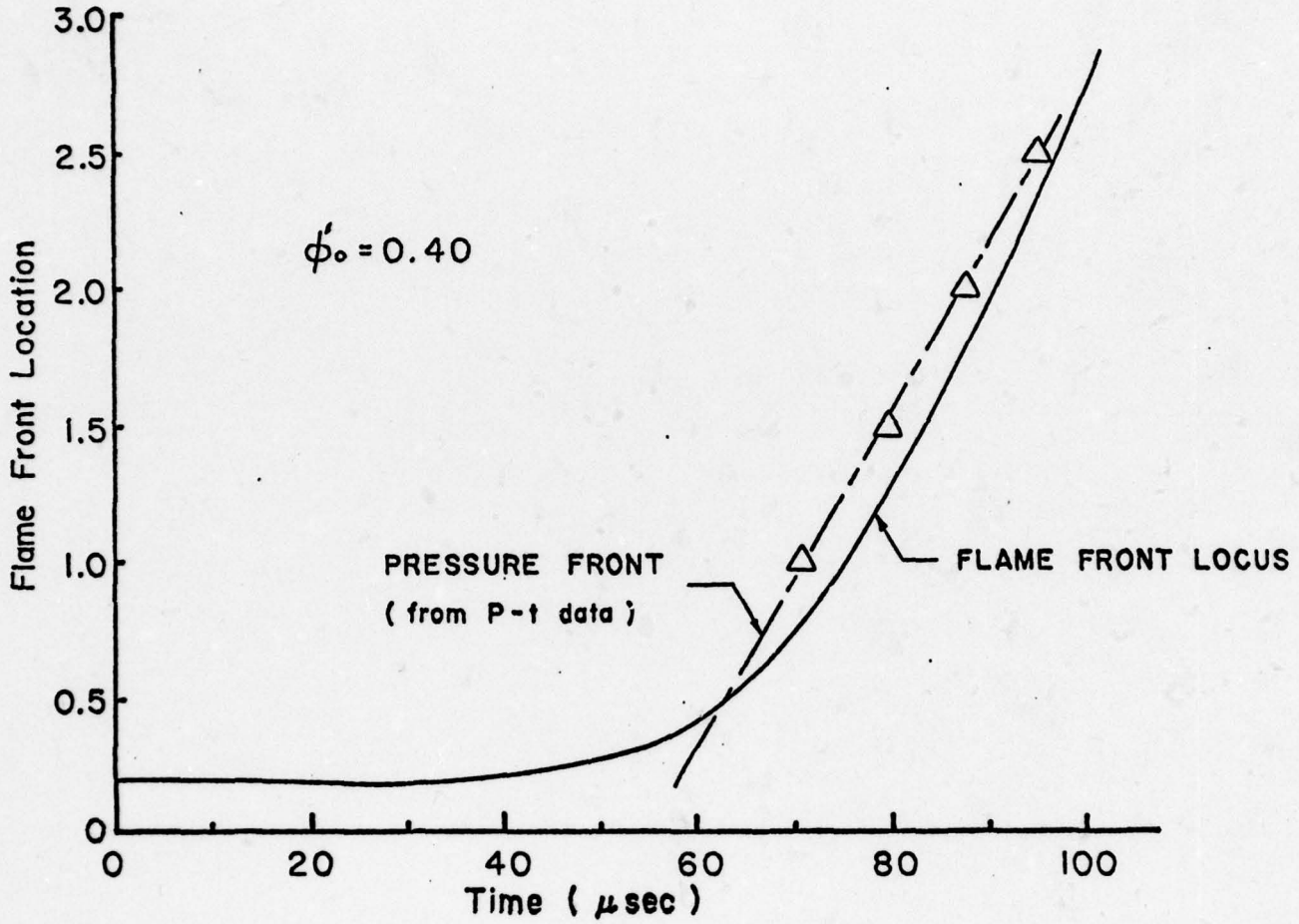


Figure 8 Flame front locus and pressure wave front, indicating conditions for possible DDT.



79-0286

Direct Detonation Initiation by Localized Enhanced Reactivity

H.O. Barthel, and R.A. Strehlow, *University of Illinois, Urbana, Ill.*

17th AEROSPACE SCIENCES MEETING

New Orleans, La./January 15-17, 1979

For permission to copy or republish, contact the American Institute of Aeronautics and Astronautics, 1290 Avenue of the Americas, New York, N.Y. 10019.

DIRECT DETONATION INITIATION BY LOCALIZED ENHANCED REACTIVITY

H. O. Barthel* and R. A. Strehlow**
Department of Aeronautical and Astronautical Engineering
University of Illinois at Urbana-Champaign
Urbana, Illinois

Abstract

The Oppenheim CLOUD program has been adapted to study the possibility of initiating detonation in a reactive mixture that contains a spherically symmetric local region of enhanced reactivity. The induction zone for the reactive mixture is modeled by an Arrhenius kinetic law. The effect of the enhancement is modeled by changing the following factors: the activation energy for the induction zone, the spatial distribution in the enhanced reactivity region, the pre-exponential coefficient and the maximum allowable rate of energy release. All these variables have been found to affect the ability of the localized rapid reaction in the central region to trigger detonation in the surrounding cloud.

Introduction

In 1970 Meyer et al.[1] discovered a mechanism for initiation of detonation in which direct initial shock heating is not the important triggering mechanism. Recently Knystautas et al.[2,3] have also shown experimentally that a properly shaped region of enhanced reactivity can cause direct initiation of detonation without the initial presence of a strong shock in the system.

This phenomenon of direct initiation of detonation by localized enhanced reactivity is very important to our understanding of the mechanisms of blast wave production in unconfined vapor cloud explosions. It is now well known that extremely high effective burning velocities must be reached if a damaging blast wave is to be generated by a premixed, unconfined cloud that is burning. Up until the discovery of this particular initiation phenomenon the mechanism of transition to such extremely high burning velocities or even to detonation under conditions of partial confinement was not understood. It was obvious from experimental evidence (the accidents themselves) that transitions were occurring under situations where the confinements were not sufficient to first produce strong shock waves. It currently appears that the direct initiation by localized enhanced reactivity that Knystautas and his co-workers have observed is the most viable mechanism for the production of extremely high burning velocities or transition to detonation in situations where only partial confinement is available.

It is also well known that constant volume explosion followed by release of the high pressure contents cannot generate shock waves that are strong enough to induce exothermic chemical reactions in hydrocarbon-air mixtures.[4] The shock wave temperatures are just too low. However, one of the mechanisms proposed by Knystautas et al.[2,3] for the production of detonation is a chemical reaction-gas dynamic process in which the intense chemical reaction in a central region generates pressure waves that interact with a neighboring region having a spatial gradient of chemical reactivity. Lee and co-workers have observed this effect experimentally. Under these conditions they postulated that the waves enhance the reactivity in the gradient region and a reactive wave can actually accelerate to detonation velocity.

This paper presents the results of a numerical study to test the possibility that such an acceleration mechanism is indeed available in a completely unconfined situation. In the idealization used here the geometry is strictly spherical and the entire system is assumed to be heated by a simple thermal explosion process having hydrocarbon-air Arrhenius kinetics as derived from shock tube measurements. In the neighborhood of the origin the system is arbitrarily given enhanced reactivity without increasing the local heat of combustion. With these conditions, the CLOUD[5,6] program is used to calculate the nonsteady development of the flow field for various assumed profiles for the central region of enhanced reactivity.

Mathematical Formulation

Our model for this study is heat addition to a perfect gas with constant gamma throughout. The fluid is initially uniform and at zero time the region of enhanced chemical reactivity is created with spherical symmetry and without disturbing the background gas. We choose to formulate the problem in Lagrangian form, for which the relevant equations are:

$$\frac{\partial v}{\partial t} = \frac{v}{r^j}\frac{\partial (u r^j)}{\partial r} \tag{1}$$

$$\frac{\partial u}{\partial t} = -v\frac{\partial p}{\partial r} \tag{2}$$

$$\frac{\partial e}{\partial t} = -p\frac{\partial v}{\partial t} + \dot{q} \tag{3}$$

$$e = \frac{pv}{\gamma - 1} \tag{4}$$

$$\frac{\partial r}{\partial t} = u \quad , \tag{5}$$

where r is the position coordinate, γ, v, u, e, p and $\dot{q}$, respectively, are the specific heat ratio, specific volume, radial velocity, internal energy, pressure, and rate of energy addition, and j = 0, 1, 2 for planar, cylindrical and spherical geometries.

*Associate Professor
**Professor, Associate Fellow AIAA

Copyright © American Institute of Aeronautics and Astronautics, Inc., 1979. All rights reserved.

We scale the problem by introducing r_o, the outer radius of the region of enhanced reactivity, introduce

$$t_o = r_o/\sqrt{p_o v_o}\ ,\quad V = \frac{v}{v_o},\quad U = \frac{u}{\sqrt{p_o v_o}},\quad E = \frac{e}{p_o v_o},$$

$$P = \frac{p}{p_o},\quad \dot{Q} = \frac{\dot{q}}{p_o v_o}\, t_o,\quad R = r/r_o \text{ and } \tau = t/t_o.$$ With these quantities, Eqs. (1)-(5) become

$$\frac{\partial V}{\partial \tau} = \frac{V}{R^j}\frac{\partial (UR^j)}{\partial R} \tag{6}$$

$$\frac{\partial U}{\partial \tau} = -V\frac{\partial P}{\partial R} \tag{7}$$

$$\frac{\partial E}{\partial \tau} = -P\frac{\partial V}{\partial \tau} + \dot{Q} \tag{8}$$

$$E = \frac{PV}{\gamma - 1} \tag{9}$$

$$\frac{\partial R}{\partial \tau} = U\ . \tag{10}$$

The energy addition term, $\dot{Q}$, is assumed to be given by

$$\dot{Q} = \frac{\Delta E}{p_o v_o}\frac{d\lambda}{d\tau}\ , \tag{11}$$

where ΔE is the heat released by a particular fuel-oxidizer system per unit volume v_o, and λ is the reaction coordinate with range $0 \le \lambda \le 1$. The ratio $\Delta E/p_o v_o$ is related to the value of M_{CJ} by the expression

$$M_{CJ}^2 = 1 + \frac{\gamma^2-1}{\gamma}\frac{\Delta E}{p_o v_o} + \left[\frac{(\gamma^2-1)}{\gamma}\frac{\Delta E}{p_o v_o}\left(2 + \frac{\gamma^2-1}{\gamma}\frac{\Delta E}{p_o v_o}\right)\right]^{1/2}. \tag{12}$$

The reaction rate $\frac{d\lambda}{d\tau}$ is assumed to be given by the Arrhenius law

$$\frac{d\lambda}{d\tau} = A_o\frac{(1-\lambda)^n}{V^{n-1}}\exp\left(-\frac{E^*}{E}\right)\ , \tag{13}$$

where E^* is the dimensionless activation energy, n is the order of the reaction and A_o is the pre-exponential factor which is assumed to depend upon both the reactive system and the enhanced chemical reactivity of the central region as follows:

$$A_o = A_1(1 + A) \qquad 0 \le R \le \beta$$

$$= A_1(1 + A\phi(R)) \qquad \beta < R \le 1$$

$$= A_1 \qquad 1 < R < \infty$$

A_1 is the dimensionless preexponential factor for the reactive system without enhancement, A is an amplifying factor which models the effect of enhanced reactivity, $\beta(<1)$ is the radius of the core over which the enhanced reactivity is uniform. In the transition region where $\beta < R \le 1$, the function $\phi(R)$ is given by

$$\phi(R) = [\cos(3\pi\psi) - 9\cos(\pi\psi) + 8]/16 \tag{15}$$

with

$$\psi = \frac{R-1}{\beta-1}\ . \tag{16}$$

This function blends very smoothly with the functions for the adjacent regions, for not only do their values match, but their first, second and third derivatives are zero at the end points and therefore also match.

With the assumption of initial uniformity, the initial conditions are:

$$R(0) = R_k \qquad k = 1,\ldots.m \tag{17}$$

$$P(R_k,0) = 1 \tag{18}$$

$$V(R_k,0) = 1 \tag{19}$$

$$U(R_k,0) = 0 \tag{20}$$

$$E(R_k,0) = 2.5 \tag{21}$$

$$\lambda(R_k,0) = 0 \tag{22}$$

Further, the boundary conditions at R = 0 for $\tau > 0$ are

$$U(0,\tau) = 0 \tag{23}$$

$$\frac{\partial P}{\partial R}(0,\tau) = 0 \tag{24}$$

$$\frac{\partial U}{\partial R}(0,\tau) \neq 0 \tag{25}$$

$$\frac{\partial E}{\partial R}(0,\tau) = 0 \tag{26}$$

$$\frac{\partial \lambda}{\partial R}(0,\tau) = 0 \tag{27}$$

The disturbance caused by the energy release will be propagated outward and the leading edge of this disturbance will be bounded by an acoustic wave or a shock wave. Ahead of this lead wave, the variables will remain at their initial values but inside they change and their values must be computed. This is true even though the entire field is assumed to be reactive with Arrhenius kinetics (Eq. 13) because at t = 0 we assume that $\lambda = 0$ everywhere and the only cases of interest to this study are those when $\lambda \ll 1$, unless the region has enhanced reactivity due to some external physical phenomenon such as flame folding, or the region has been shock heated to a condition that triggers rapid reaction. Essentially this means that the nature of our approach to the problem in effect renders the surroundings nonreactive during the observation time. This will be discussed further in the results section.

Computation

The computer program for the calculations is based upon the CLOUD program of Oppenheim[5] as subsequently modified by Adamczyk.[6] The latter simply added an energy source term to the energy equation but retained the other features of the original

CLOUD program, including the finite difference integration scheme and artificial viscosity to smear out shock fronts or steep velocity gradients. Of course, we replaced Adamczyk's energy addition law by the Arrhenius law detailed in Eqs. (11) and (13).

Our first attempts at running this program produced very long run times which were caused by extremely small time increments resulting from the Courant stability requirement applied to the steep gradients that developed. To shorten the run time we subsequently introduced a minimum time increment which we would allow and, as one would expect, stability problems appeared. This instability would manifest itself when new radii or R values calculated by using Eq. (10) would not agree with radii calculated from the new volume or V values based upon mass conservation. The problem would arise when the rate of energy addition had large spatial gradients, which in turn caused the flow velocity, U, to change rapidly, so that the average value of U used in the program did not advance R sufficiently.

This instability problem was overcome by adding one predictor-corrector type iteration step to the calculation. The order of procedure in the CLOUD program is to use Eq. (7) and then Eq. (10) to advance the velocity and position at half points in the space-time grid, then to use Eq. (6) to advance the specific volume at integer points in the space-time grid. After advancing the specific volume at point i, we recalculated the value of position at i + 1/2 by using mass conservation with the tentative value of specific volume, then recalculated the specific volume using Eq. (6) from this corrected value of position.

Once the minimum time increment is reached in the calculation, subsequent calculations proceed at this time increment unless the time increment as calculated from the Courant stability criterion again becomes larger. We have completed perhaps 20 computer runs without difficulty, and we believe that in some runs that this minimum time increment may have been as much as ten times the value permitted by the Courant condition.

The Role of the Parameters

As formulated, there are eight dimensionless parameters which appear in the problem, namely, n, γ, β, $\Delta E/p_o v_o$, E^*, A, A_1 and $\dot{Q}_m$, where $\dot{Q}_m$ is the maximum energy addition rate. The parameter n is the order of the reaction and has a characteristic value for a specific system of reactants. The specific heat ratio, γ, is specific for each system. The parameter β defines the extent of the flat central core for the region of enhanced reactivity and therefore the relative steepness of the distribution in the transition region. The parameter $\Delta E/p_o v_o$ represents a dimensionless combustion energy and, as mentioned earlier, determines the value of shock Mach number which would finally be attained if a successful transition to a Chapman-Jouguet detonation occurs. The dimensionless activation energy, E^*, determines the relative ease of reaction with temperature and is linked to A and A_1, for the larger the value of E^*, then the larger the product of A and A_1 must be to start the reaction. The amplification factor, A, essentially describes the "effectiveness" of the enhanced reactivity in producing the reaction in the core region.

The remaining two parameters, A_1 and $\dot{Q}_m$, are both essentially the ratio of two time scales, with one time scale always being related to the time for a signal to propagate across the core and the other being a characteristic time for reaction. The role of A_1 is to determine the incubation time in our model while $\dot{Q}_m$ determines whether transition to detonation will occur, since another way to interpret its meaning is that it represents the ratio of maximum rate of energy input to the rate at which energy can be propagated outward through acoustic waves. This interpretation implies a critical value of $\dot{Q}_m$ below which transition will not occur and above which it will occur. Further, if A_1 is too small, the required critical $\dot{Q}_m$ may be greater than the system is capable of producing and hence implies that there is a critical value of A_1, say A_1^*, below which the transition to detonation cannot occur. Consequently, for a given system with localized enhanced reactivity there is a minimum core size which is necessary in order to achieve transition to detonation. Further, for A_1 values larger than A_1^*, the system is not actually constrained as we required in the calculations and thus would achieve values of $\dot{Q}_m$ larger than the critical values required for transition to detonation. These considerations are summarized qualitatively in Fig. 1.

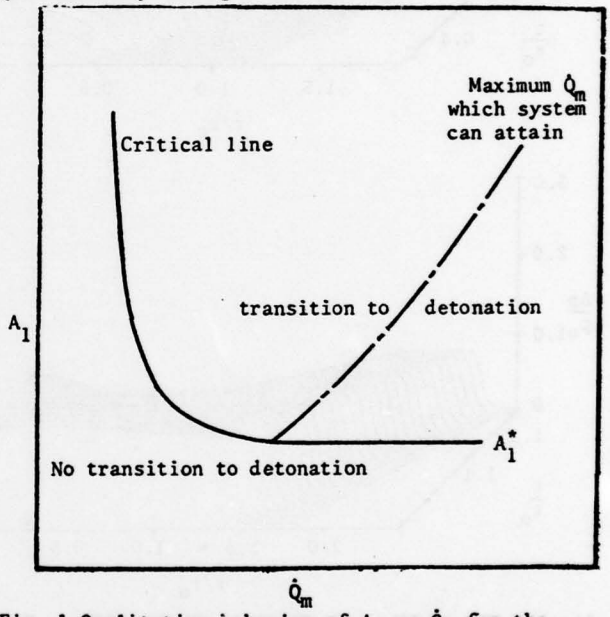


Fig. 1 Qualitative behavior of A_1 vs $\dot{Q}_m$ for the critical line and maximum energy rate line.

Numerical Results

Our computational efforts have mainly been based on the following values for the parameters: n=2, γ=1.4, β=.2, $\Delta E/p_o v_o$=20, E^*=168 and A=10^8. We have assumed values of A_1 on the order of 10^{18} and computed the behavior for various values of $\dot{Q}_m$ which are set by the program, after we provide a multiplier according to how large we want $\dot{Q}_m$ to be compared to the maximum energy addition rate when the minimum time increment is determined. The E^* value is appropriate for propane or ethylene which have activation energies on the order of 40 kcal/g mole and the $\Delta E/p_o v_o$ value at constant volume will

produce a pressure rise to initial pressure ratio equal to eight or an M_{CJ} value of approximately 5.43.

In Fig. 2 the pressure-position behavior at various times is plotted for $\dot{Q}_m$ = 14.9 and $A_1 = 6.96 \times 10^{18}$. Clearly this case failed, for the lead wave reached a pressure rise ratio of approximately 1.6 near the edge of the enhancement zone at R = 1 and then started to decay. The numerical output reveals that outside the enhanced region the reaction takes place so slowly that the energy addition does not overcome the effect of the spherical divergence, so the wave decays.

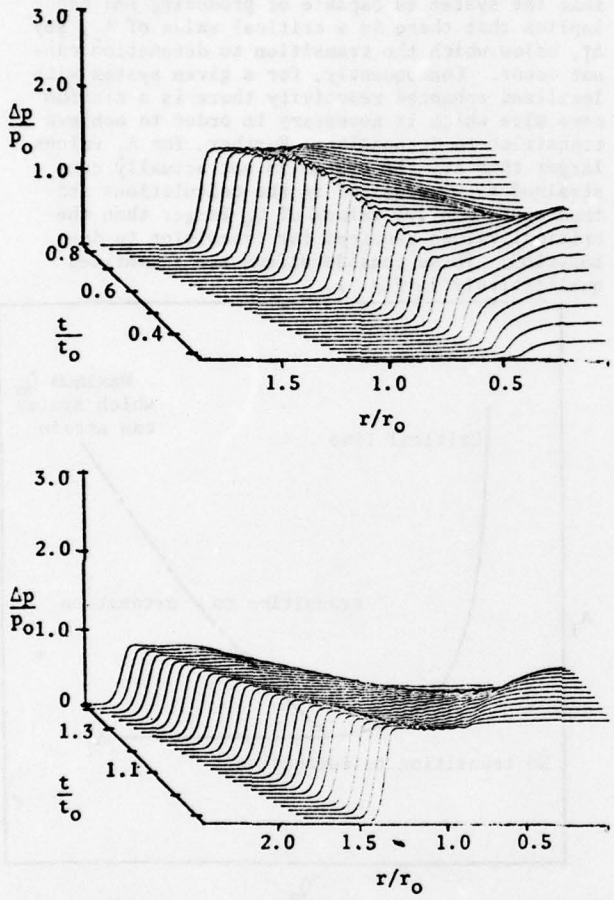


Fig. 2 Pressure rise ratio vs dimensionless radius at different dimensionless times for a $\dot{Q}_m$ value at which transition to detonation failed. Top, during time interval while enhanced region reacts; Bottom, during time interval while very little reaction occurs anywhere. $A_1 = 6.96 \times 10^{18}$. $\dot{Q}_m = 14.9$.

This result should be contrasted with Fig. 3 which shows the pressure-position behavior at various times for $\dot{Q}_m$ = 28.9 and the same A_1. Now, while there appears to be a momentary hesitancy as the lead wave passes R = 1, the strength continues to grow, albeit rather slowly, for at the end time shown, the pressure rise ratio is only about 25% of the pressure rise ratio for a Chapman-Jouguet wave for this system. The important fact is that the gas is reacting outside the region of enhancement to increase the strength of the lead wave.

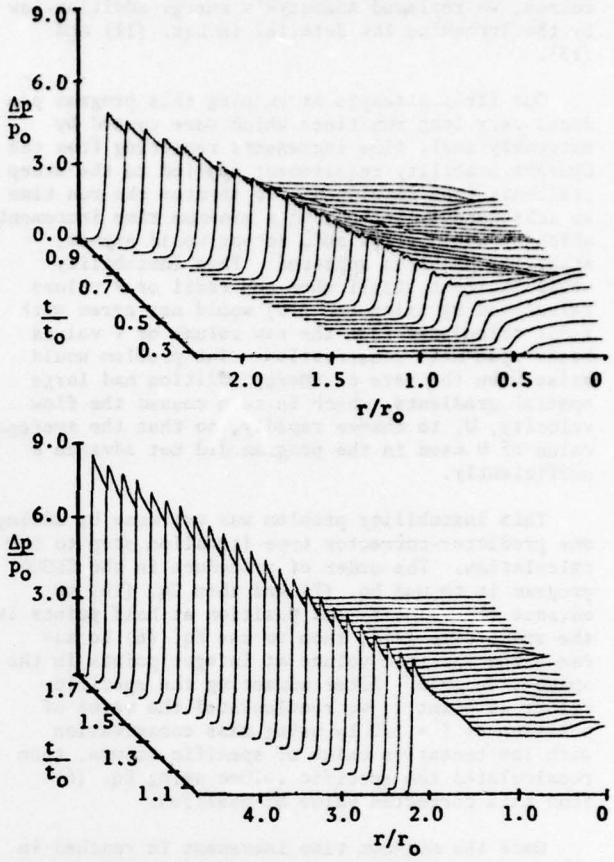


Fig. 3 Pressure rise ratio vs dimensionless radius at different dimensionless times for a $\dot{Q}_m$ value at which transition to detonation is occurring very slowly. Top, during time interval while enhanced region reacts; Bottom, during time interval while reaction occurs outside enhanced region. $A_1 = 6.96 \times 10^{18}$. $\dot{Q}_m = 28.9$.

We have similar results also for $A_1 = 6.96 \times 10^{17}$. For $\dot{Q}_m$=26.8 the wave failed, while for $\dot{Q}_m$=53.6 the wave strength was still growing at the end of the computer run.

Additional features we noticed in the computer outputs include the following: At the larger value of A_1 the uniform core reacts essentially at constant volume, but at the smaller value of A_1 the reaction moves out progressively in the uniform core. For both values of A_1, when $\dot{Q}_m$ is low the reaction region is very diffuse and may involve many "cells", perhaps as many as one hundred while for larger $\dot{Q}_m$ the reaction region is much thinner, being of the order of ten cells. Also the larger the value of $\dot{Q}_m$, the more rapidly the strength of the lead wave approaches the value for a CJ wave. This behavior is shown, for example, by these data for cases with $A_1 = 6.96 \times 10^{18}$. With $\dot{Q}_m$=28.9 the maximum pressure ratio has risen to only 9.72 at τ=1.89 while for $\dot{Q}_m$=149.3 the maximum pressure ratio has risen to 19.1 at τ=1.07.

For $A_1 = 6.96 \times 10^{18}$, the "incubation" time, defined as the time for a cell to reach a pressure ratio of 1.08, is .275 while for $A_1 = 6.96 \times 10^{7}$ the incubation time is 4.42, more than 15 times

greater, so this is a nonlinear effect. Consequently, further reduction in A_1 values would be expected to increase incubation times enormously.

We close by noting that typical values of λ in the region outside the leading wave are of the order of 10^{-13} at the end of the computer run. These values are so small that the surrounding region effectively is nonreactive during the time period of interest.

Discussion

Obviously, the results presented here are largely preliminary. Nonetheless, these results confirm that direct initiation with localized enhanced reactivity is possible in our model for certain combinations of parameter values and a particular distribution in the enhancement transition region. Further, they seem to confirm that the transition region is necessary but indicate nothing concerning the optimum shape of that region. Clearly, they show that some minimum wave strength is needed at the edge of the enhancement region if the reaction wave is to continue to grow in amplitude as it moves outside the enhancement region. Thus, even at this early stage of development, this concept shows that limiting the maximum local rate of energy addition is a possible method to prevent transition to detonation by localized enhanced reactivity.

Based on these preliminary results, it is contemplated that a complete parametric study will be performed.

Acknowledgment

The work reported here was supported by AFOSR Grant 77-3336, Dr. B. T. Wolfson technical monitor.

References

1. Meyer, J. W., Urtiew, P. A., and Oppenheim, A. K., "On the inadequacy of gasdynamic processes for triggering the transition to detonation," Combustion and Flame 14, 13 (1970).

2. Knystautas, R., Lee, J. H., and Yoshikawa, N., "Initiation of Detonation by Flash Photolysis," Paper presented at the Sixth Internation Symposium on Gasdynamics of Explosions and Reactive Systems, Stockholm, August 1977. In press, Acta Astronautica (1979).

3. Knystautas, R., Lee, J. H., Moen, I., and Wagner, H. Gg., "Direct Initiation of Spherical Detonation by a Hot Turbulent Gas Jet," 17th Symposium (International) on Combustion, Leeds, England, 1978. In press (1979).

4. Cesarone, R. J. "Direct Initiation of Dettonation by Nonideal Blast Waves," M.S. Thesis, University of Illinois, 1977. Interim Technical Report AFOSR-TR-0842; AAE 77-4, UILU Eng 77-0504.

5. Oppenheim, A. K., "Elementary Blast Wave Theory and Computations," Proceedings of the Conference on Mechanisms of Explosion and Blast Waves, Paper No. 1, Yorktown, VA (1973).

6. Adamczyk, A. A., "An Investigation of Blast Waves from Non-Ideal Energy Sources," Ph.D. Thesis, University of Illinois, Urbana, IL (1975).